

**UNCLASSIFIED**

---

**AD 274 197**

*Reproduced  
by the*

**ARMED SERVICES TECHNICAL INFORMATION AGENCY  
ARLINGTON HALL STATION  
ARLINGTON 12, VIRGINIA**



---

**UNCLASSIFIED**

NOTICE: When government or other drawings, specifications or other data are used for any purpose other than in connection with a definitely related government procurement operation, the U. S. Government thereby incurs no responsibility, nor any obligation whatsoever; and the fact that the Government may have formulated, furnished, or in any way supplied the said drawings, specifications, or other data is not to be regarded by implication or otherwise as in any manner licensing the holder or any other person or corporation, or conveying any rights or permission to manufacture, use or sell any patented invention that may in any way be related thereto.

#274197

CATALOGED BY ASTIA  
AS AD NO. \_\_\_\_\_

**First Quarterly Technical Progress Report  
on Design and Development of a Liquid Metal Cell  
for the Period 1 January 1962 - 31 March 1962**

**Allison EDR 2678**

**15 April 1962**

**INDEX**  
**N-62-3-1**

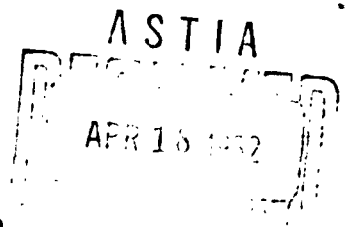
**Flight Accessories Laboratory  
Aeronautical Systems Division  
Air Force Systems Command  
Wright-Patterson Air Force Base, Ohio**

**Project No. 3145; Task No. 60013**

37800

**(Prepared under Contract No. AF33(657)-7847  
by Allison Division, General Motors Corporation,  
Indianapolis, Indiana**

**Authors: Dr. B. Agruss and H. R. Karas)**



---

## FOREWORD

This report was prepared by the Research Group of the Allison Division of General Motors Corporation on Air Force Contract AF33(657)-7847, Task No. 60813, Project No. 3145. The work was administered under the direction of the Flight Accessories Laboratory, Aeronautical Systems Division. Mr. F. J. Brock is the task supervisor for ASD.

The work began on 2 January 1962 on a basic contract to result in the design and development of a stack of potassium-mercury liquid metal cells having a power output of 310 watts at approximately 3.5 volts. The construction and operation of this stack assembly is to demonstrate the feasibility of the liquid metal cell as a source of future space power. This report is being written to fulfill part of the contract commitment.

The Liquid Metal Cell Project is managed by Dr. B. Agruss, Section Head, Applied Chemistry. Dr. Agruss and H. R. Karas are responsible for the work at Allison. Management direction at Allison includes Mr. T. F. Nagey, Director of Research, and Dr. R. E. Henderson, Chief of Applied Physics.

---

## ABSTRACT

Electrochemical, physical, and chemical characteristics of potassium, mercury, and potassium-mercury amalgams lend themselves to the successful operation of a liquid metal cell for space power. Construction of single liquid metal cells and a three-cell unit is complete and testing is in progress. Preliminary design work to show that the cells can be combined into a system which will function as a battery is nearly complete. Photographs and detailed drawings of the units used for the cell, instrumentation, feed system, etc, are shown.



## TABLE OF CONTENTS

<u>Section</u>	<u>Title</u>	<u>Page</u>
I	Introduction . . . . .	1
II	Theory . . . . .	3
III	Apparatus and Reactants . . . . .	9
	Choice of Material . . . . .	9
	Construction . . . . .	27
IV	Experimental Results . . . . .	49
	Preliminary Tests . . . . .	49
	Stability Tests . . . . .	49
	Power Output Tests . . . . .	50
V	Preliminary Design of a Multicell Stack . . . . .	53
	Multicell Unit Fabrication . . . . .	61
VI	Technical Position . . . . .	63
VII	Work Plan for Next Report Period . . . . .	65
VIII	References . . . . .	67

## LIST OF ILLUSTRATIONS

<u>Figure</u>	<u>Title</u>	<u>Page</u>
1	EMF vs Composition for K-Hg System. . . . .	7
2	Schematic Diagram of an Operating Cell . . . . .	8
3	Density of Amalgams as a Function of Composition. . .	18
4	Amalgam Viscosity Versus Composition. . . . .	19
5	Phase Diagram of KOH System. . . . .	20
6	Phase Diagram of KOH-KBr System. . . . .	25
7	Phase Diagram of KOH-KI System. . . . .	25
8	Phase Model of KOH-KBr-KI System . . . . .	26
9	Bottom Half of Circular Cell. . . . .	29
10	No. 5186 Matrix and A-402 Gasket . . . . .	30
11	Top Half of Circular Cell . . . . .	31
12	Cell in Press . . . . .	32
13	Experimental Setup. . . . .	33
14	Detail of Bottom Half of Circular Cell. . . . .	34
15	Detail of Top Half of Circular Cell. . . . .	35
16	Detail of Cell Profile and Intermediate Type Cells . . .	36
17	Level Sensor . . . . .	37
18	Rectangular Cell with Matrix in Place. . . . .	37
19	Rectangular Cell Outside of Press. . . . .	38
20	Detail of Rectangular Cell . . . . .	39
21	Cell Stack. . . . .	40
22	Press Assembled. . . . .	41
23	Press—Top Plate . . . . .	42
24	Press—Bottom Plate. . . . .	43
25	Press—Intermediate. . . . .	44
26	Press—Transite Insulating Plate . . . . .	44
27	Press—Small Parts . . . . .	45



<u>Figure</u>	<u>Title</u>	<u>Page</u>
28	Feed Pot . . . . .	46
29	Impregnation Tank . . . . .	46
30	Matrix Design. . . . .	48
31	Shorted Matrix . . . . .	50
32	Top View of 310-Watt Stack of 3-in. Cells. . . . .	54
33	Detail of Mercury Weirs . . . . .	55
34	Schematic of Feed System for Liquid Metal Cell Stack . . . . .	56
35	Detail of Potassium Weir. . . . .	58
36	Schematic of Exterior Electrical Connections. . . . .	59
37	Program Schedule . . . . .	63



## LIST OF TABLES

<u>Table</u>	<u>Title</u>	<u>Page</u>
I.	Important Properties of Metals Useful in Liquid Metal Cell Construction . . . . .	10
II.	Physical Characteristics of No. 5186 Alumina . . . . .	15
III.	Physical Characteristics of A-402 Impervious Alumina . . . . .	15
IV.	Characteristics of LA Series Ceramics . . . . .	16
V.	Properties of Mercury Metal . . . . .	21
VI.	Properties of Metallic Potassium . . . . .	22

## LIST OF SYMBOLS AND DEFINITIONS

<u>Symbol</u>	<u>Description</u>
A	Area or representation of a liquid metal
B	Representation of a liquid metal
a	Activity
D	Diameter of smallest pore filled at pressure p
E, emf	Reversible electrical potential
F	Faraday
$\Delta G$	Free energy
$\overline{\Delta G}$	Partial molar free energy
$\Delta H$	Enthalpy
I	Current
K	Thermodynamic equilibrium constant
l	Path length
N	Mole fraction
n	Number of electrons taking part in a reaction
p	Applied pressure
R	Gas constant or electrical resistance
$\Delta S$	Entropy
(s)	Solid
T	Absolute temperature
V	Cell voltage
$V_o$	Open circuit voltage
$\gamma$	Activity coefficient
$\rho$	Resistivity
$\sigma$	Surface tension
$\theta$	Wetting angle
x, y	Stoichiometric ratios



### Definitions

Cell---A single cell consisting of the anode chamber, electrolyte matrix, and cathode chamber

Cell Unit---A number of cells in series to provide a basic package of given operating voltage

Cell Stack---A group of cell units arranged in such a manner as to provide a package of given wattage

## I. INTRODUCTION

A comprehensive survey was made of the fuel cell literature.<sup>1\*</sup> From this survey it was noticed that very little work was being done on regenerative systems—a surprising observation considering the preponderance of thermal energy available from both solar and nuclear sources. It was then suggested that thermal and electrochemical regenerative systems should be studied.<sup>2</sup> Pursuing these leads further, it was decided to determine the problems associated with such systems and what inorganic compounds would lend themselves to thermal regeneration. A survey of the literature for thermally decomposable inorganic compounds<sup>3</sup> revealed only about 20 compounds suitable for thermally regenerative systems based on more or less practical criteria, while another evaluation<sup>4</sup> based on thermodynamic and kinetic data produced only two suitable reactions for inorganic compounds. A general systems analysis<sup>5</sup> revealed that the greatest improvement in efficiency of regenerative systems could be accomplished by reductions in polarization and electrolyte resistance losses. It is known that the kinetics of liquid metal electrodes in contact with fused salts is extremely rapid.<sup>6</sup> Also, the conductivity of fused salts is possibly two to five times greater than the conductivity of the best aqueous electrolytes.

With these improvements as the goal, the liquid metal cell is being developed at Allison. The program consists of using two liquid metals—potassium and mercury (which are most amenable to use in a nuclear regenerative system)—and a series of molten salts containing the common cation, potassium. This system,  $\text{K-Hg}|\text{KOH-KBr-KI}|\text{Hg-K}$ , will be used in the construction of the 310-watt stack for this contract commitment.

---

\*Superscripts refer to references in Section VIII.

## II. THEORY

### ELECTROCHEMICAL THEORY

When metals react to form alloys, solutions, and compounds, an exchange of energy takes place which may manifest itself in the form of heat. These reactions can be analyzed by standard thermodynamic principles.<sup>7</sup> For instance, the heat of the reaction may be expressed as

$$\Delta H = \Delta G + T \Delta S. \quad (1)$$

Two methods—calorimetric or electrochemical—are used to evaluate the terms of Equation (1). The former measures enthalpy,  $\Delta H$ , and entropy,  $\Delta S$ , from which the free energy,  $\Delta G$ , can be calculated. The latter measures  $\Delta G$ , and  $\Delta H$  is calculated according to the Gibbs-Helmholtz equation:

$$E = - \frac{\Delta H}{nF} + T \left( \frac{dE}{dT} \right) \quad (2)$$

where

$$\Delta S = - nF \left( \frac{dE}{dT} \right) \quad (3)$$

and

$$\Delta G = - nFE. \quad (4)$$

The free energies involved can be measured in galvanic cells in which the anode is formed of the more electronegative metal and the cathode is formed of the alloy. The cation of the electrolyte is the ionized form of the anode metal. The cell is represented schematically as



Therefore, in a cell constructed as in (S), comprising two liquid metal electrodes and a molten electrolyte, the voltage will be governed by Equation (6) and the current by

$$I = \frac{V_o - V}{R} \quad (12)$$

where  $V_o$  is the open circuit voltage from Equation (6),  $V$  is the operating voltage at current  $I$ , and  $R$  is the cell resistance.

Because liquid metal electrodes are used, electron transfer and metal diffusion should be very rapid. This means that the cell should operate with little or no polarization loss; the electrical losses should be limited to  $IR$  (i. e., ohmic resistance) losses entirely. The exchange currents at metal electrodes in molten salts can be extremely high,<sup>6</sup> which permits high current densities with very small amounts of activation polarization. Also, the cation of the molten electrolyte has a transference number of nearly unity; hence, there can be no concentration polarization in the electrolyte. There can be some concentration polarization at the alloy electrode-electrolyte interface at high current densities where metal A can be discharged faster than surface tension effects and diffusion can remove it, resulting in a thin, high alloy concentration layer. Because of the extremely rapid diffusion rates at these high temperatures in liquid metals and the stirring effect caused by the change in surface tension, this polarization could occur only at high current densities, but here the  $IR$  drop would greatly overshadow the small polarization effect. Hence, the only significant voltage loss in a liquid metal cell of this type should be the  $IR$  loss in the electrolyte.

These  $IR$  losses, also, are minimal and much lower than those encountered in aqueous systems because molten salts have conductivities of the order of 2-5 mhos, while the best aqueous electrolyte conductivities are in the range of 0.5-0.9 mho.

Based on carefully screened data,<sup>8</sup> Figure 1 shows the effect of a change in amalgam composition as it would affect the open circuit voltage of the liquid metal cell. With the cell in operation, the load voltage would be a function of the current drawn and the electrolyte-matrix resistance as given in Equation (12).

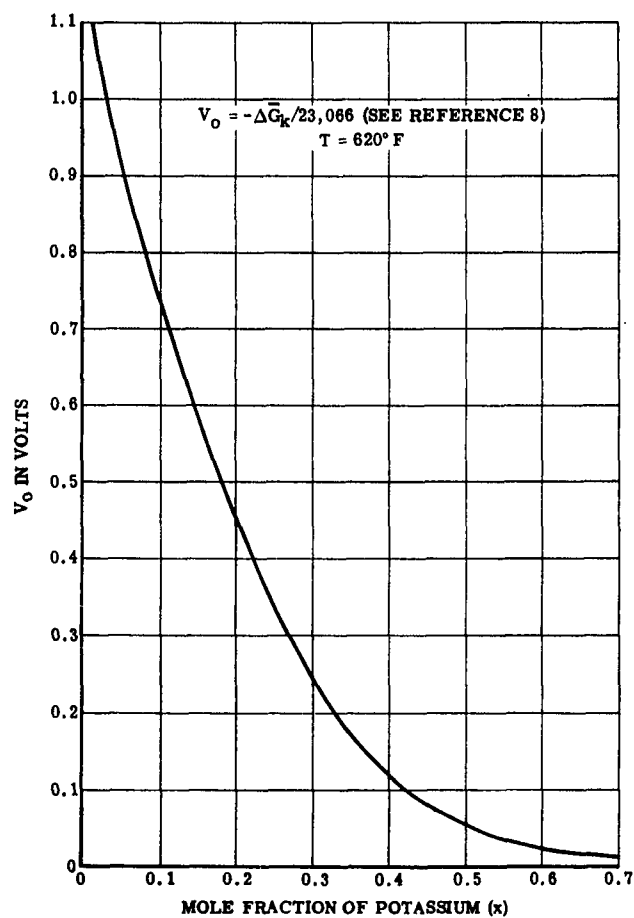
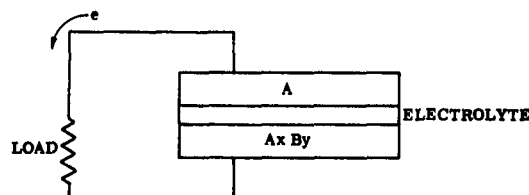


Figure 1. EMF vs Composition for K-Hg System

Actual operation of a single cell within the stack is shown schematically in Figure 2.



**Figure 2. Schematic Diagram  
of an Operating Cell**

In Figure 2, A and  $A_x B_y$  are chambers containing A and  $A_x B_y$ , respectively, separated by a porous ceramic matrix. The electrolyte is a molten salt (consisting of a cation of metal A and some anions) soaked into the matrix. (This electrolyte is chosen mainly on the criteria of proper melting point range, lack of reaction with the liquid metals, matrix, or container, and the absence of thermal decomposition.) As the cell commences operation, the following reaction takes place:

1. A gives up an electron and becomes the ion  $A^+$ .
2. The ion  $A^+$  migrates into the electrolyte and displaces a cation,  $A^+$ , of the electrolyte.
3. The electron passes through the load in the external circuit furnishing electrical power and unites at the electrolyte  $A_x B_y$  interface with the cation,  $A^+$ , forming the neutral atom A.
4. A reacts with the alloy  $A_x B_y$ , forming the alloy  $A_x' B_y$ .

The amount of current or voltage available from a cell of this type is a function of the electrode area, electrolyte-matrix resistance, and other intracell resistances. As current is drawn, the potassium-rich amalgam in the anode compartment loses potassium to the cathode chamber and, consequently, becomes richer in mercury. The mercury-rich amalgam in the cathode compartment takes on more and more potassium. It can be seen from Figure 1 that the expected emf of the cell will be decreasing as current is drawn. By feeding fresh amalgam into the cell halves the composition levels are maintained and a steady emf can be drawn. Such a feed and effluent system will be incorporated in the 310-watt cell stack.



### III. APPARATUS AND REACTANTS

#### CHOICE OF MATERIAL

##### Metals

The following criteria should be considered in the choice of containment metals for a cell system:

1. Compatibility with mercury and alkali metals
2. Thermal expansion
3. Density
4. Cost
5. Machinability and joining

The Liquid Metals Handbook<sup>9</sup> lists the results of tests run on the resistance of materials to attack by mercury and by sodium and sodium-potassium alloys. It is pointed out that while there are some materials which are resistant to mercury in static systems, great care must be used in selection since dynamic mercury systems significantly affect the corrosion properties of metals. At low flow rates (as would be encountered in a liquid metal cell), corrosion is very serious. Therefore, most reliance was placed on those tests which were run in dynamic rather than static systems.

The metals which would seem to lend themselves most readily to use in the liquid metal cell system are divided into two classes---ferrous and nonferrous. The ferrous metals of primary interest would be (1) the low carbon steels, which show good resistance in dynamic systems from temperatures of 673 to 923°K depending on the particular formulation, (2) stainless steels of the ferritic type, and (3) a few of the proprietary alloys. Nonferrous metals showing promise would include tungsten, listed as having good properties to 873°K, molybdenum to 873°K, and chromium to 823°K (as measured in a static system). The literature also indicates that low carbon steels are listed as having good resistance up to 673°K, while the addition of small amounts of chromium, silicon, titanium, and molybdenum can increase this resistance up to 873°K.<sup>9</sup>



The ferritic steels, which are high chromium stainless types with little or no nickel present, showed good results in static tests but were not tested in dynamic systems. These steels would comprise the 400 series stainless steels. The 300 series stainless or austenitic steels which are high in nickel and chromium showed poor resistance to attack by mercury in dynamic systems. As to the attack by sodium or sodium-potassium alloys, carbon steels are listed as having good resistance to 723°K, while the ferritic stainless steels show good resistance up to 903°K. Reference 9 lists the possibilities of corrosion inhibitors being added directly to the mercury to reduce attack on ferrous alloys, but at this time the effect of these additives on the operation of the liquid metal system is uncertain.

The nonferrous metals previously listed show good resistance to both the sodium-potassium alloys and to the pure mercury. With the exception of chromium, these tests were in dynamic systems.

Table I is a compilation of the important properties of metals useful in constructing the liquid metal cell.<sup>10,11</sup>

TABLE I

Important Properties of Metals Useful in Liquid Metal Cell Construction

<u>Material</u>	<u>Specific Gravity (gm/cm<sup>3</sup>)</u>	<u>Thermal Expansion Coefficient, [cm/cm/°K (× 10<sup>6</sup>)]</u>	<u>Melting Point (°K)</u>
1% Carbon Steel	7.83	12.0 (473-573°K)	1703
410 Stainless Steel	7.75	9.9 (293-873°K)	1723
Tungsten	19.3	4.5 (273-573°K)	3683
Molybdenum	10.2	5.5 (298-773°K)	2898
Chromium	7.19	6.2 (not given)	2163
Alumina	Depends on porosity	8.7 (298-1173°K)	2323
Magnesia	Depends on porosity	13.5 (not given)	3073

Chromium, molybdenum, and tungsten would be very desirable materials to use in some respects. The specific gravity of tungsten, the difficulties of joining tungsten, molybdenum, or chromium, added to the fact that the 410 stainless steel has a thermal expansion coefficient close to that of alumina makes the use of the 410 stainless material desirable at this time from the standpoint of service, availability, price, and weight. This does not preclude the use of any of the materials listed in Table I at a later date, or the use of materials for which compatibility data are not now available. The use of Kovar, for example, would be highly desirable because the thermal expansions of Kovar and alumina are almost identical. Unfortunately, proper compatibility information is not presently available on Kovar or on many other alloys which show a good potential for use in this system. All of the materials listed in Table I are satisfactory from the standpoint of melting point.

#### Ceramics for Matrices and Insulators

The main criteria in the choice of ceramic materials would be:

1. Compatibility with the mercury-potassium amalgam and electrolyte systems
2. (For matrices) Apparent porosity, pore size, and distribution of the pores among the three possible types---pores open on both ends, pores open on one end, and pores closed on both ends. The maximum porosity attainable would be desirable because this would lend itself to absorption of the greatest amount of electrolyte in the pores open on both ends. But yet, a retention of the electrolyte under a differential head is important and, for this reason, it would be critical to control the pore size so that maximum electrolyte retention can be attained.



ALISON

3. Availability
4. Stability against thermal shock (the chief failing of dense MgO)
5. Cost

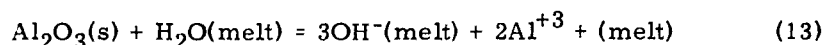
Compatibilities with mercury<sup>9</sup> are good up to temperatures of 873°K. Compatibilities in alkali metals are as follows: For alumina,  $\text{Al}_2\text{O}_3$ ---good characteristics are attained up to 773°K; beryllia,  $\text{BeO}$ ---good up to 823°K; and magnesia,  $\text{MgO}$ ---good up to 473°K, with the area beyond that unknown. (It should be remembered that the foregoing description applies to the pure mixture of alkali metals and not to an alkali metal amalgam, where the attack would be expected to be slower.)

While it is generally understood that an oxide-type ceramic will be required for durability as a matrix in the liquid metal cell, those few showing good compatibility with the metal systems must be further reduced from an availability standpoint. Alumina is the only oxide ceramic readily available at this time in a wide range of porosities, pore sizes, and size of available pieces. Magnesia is also available; however, the sizes available and fabrication experience are not as comprehensive. Beryllia, calcia, zirconia, etc, are relatively unavailable for a project of this scope. Therefore, ceramic materials considered for the basic cell construction will consist of sintered porous alumina and sintered porous magnesia.

Ryshkewitch<sup>12</sup> states that potassium induces some attack on alumina, and Reference 9 speaks of the attack of alkali metals on aluminas in which silica,  $\text{SiO}_2$ , is used as a binder.

Smith<sup>13</sup> discusses the corrosion of ceramics in fused hydroxides (a constituent of the electrolyte system used in the liquid metal cell). Smith points out the following:

1. The oxide-type ceramic has only a negligible tendency to capture an oxide ion from a hydroxyl ion in the salt and, therefore, should stand up fairly well. Aluminum oxide, being more amphoteric than magnesia, should be more readily attacked, but there are definite advantages to using alumina.
2. Calcia is appreciably attacked by molten sodium hydroxide at 811°K, but other tests indicate that the attack is relatively slow at a temperature of 623°K.
3. Three oxides---those of magnesium, zinc, and thorium---have been tested at substantial temperatures without giving evidence of reaction.
4. In spite of the fact that tests indicate that aluminas can be attacked, other tests under purportedly the same conditions indicate that aluminas stand up fairly well. Reference is made to cases of day-to-day use of aluminas in fused hydroxides in which attack is negligible.
5. Probably the two biggest factors in determining whether there is attack are the presence of water and the presence of a silica binder. Silica binder is listed by Smith<sup>13</sup> as being readily attacked by fused hydroxides. The attack by water would take place according to Equation (13).



Smith further states that ceramics impregnated with a hydroxide will disintegrate when washed with water since the hydroxide quickly forms hydrates or hydrated carbonates with appreciable volume expansion. As to the effect of alkali halides used in the electrolyte mixture, Ryshkewitch<sup>12</sup> states that there is no recognizable corrosive action on sintered alumina at temperatures of 2273°K.



To determine the compatibility characteristics of various materials produced by different manufacturers, the Allison Research Laboratories ran a series of compatibility studies in the electrolyte systems being considered for use in the liquid metal cells. Up to 30 different types of porous and impervious aluminas and magnesias were run. On the basis of these test results and availabilities, the following aluminas are considered worthy of use:

- No. 5186—a porous alumina, readily available, using a small amount of silica as binder
- LA-830, 831, or 832—a series of very high purity aluminas utilizing no binder
- A-402—a dense, impervious alumina utilizing no binding materials

The LA materials have just recently been made available and are still considered as a laboratory-type ceramic rather than a production type. No noticeable effect on strength of the ceramic specimens was noted after submersion periods of 336 hours in the electrolyte systems.

Tables II, III, and IV list some of the physical characteristics of No. 5186 alumina, A-402 impervious alumina, and the LA series ceramics, respectively.

The LA series of ceramics (Table IV) is a new laboratory development, and no physical data are available at the present time. It is known that this is a higher purity alumina than the No. 5186, using no silica as a binder. The apparent porosity is 40-45 percent and the pore size is closely controlled.

The apparent porosity is determined by dividing the actual density of the material by the density ( $3.97 \text{ gm/cm}^3$ ) of the pure oxide. The apparent porosity represents the three possible types of pores—those open on both ends, open on one end, and totally enclosed. The pores that are open on both ends or that are open on one end can be determined by an absorption method.<sup>16</sup>

TABLE II

Physical Characteristics of No. 5186 Alumina<sup>14</sup>

## Typical Chemical Analysis

Al <sub>2</sub> O <sub>3</sub>	98.85%	CaO	0.01%
SiO <sub>2</sub>	0.70%	MgO	0.02%
Fe <sub>2</sub> O <sub>3</sub>	0.11%	TiO <sub>2</sub>	0.02%
Na <sub>2</sub> O	0.28%	K <sub>2</sub> O	0.01%

Bulk Density---3.0 gm/cm<sup>3</sup>

Temperature of Maximum Use---2008-2038°K

Modulus of Rupture

Room Temperature---3160 psi

1273°K---2470 psi

Thermal Expansion--- $10 \times 10^{-6}$  (303-1773°K)

Apparent Porosity---24%

TABLE III

Physical Characteristics of A-402 Impervious Alumina<sup>14</sup>

## Typical Chemical Analysis

Al <sub>2</sub> O <sub>3</sub>	99.0%	CaO	0.3%
MgO	0.3%	SiO <sub>2</sub>	0.2-0.4%
Fe <sub>2</sub> O <sub>3</sub>	0.03%	Alkali (Na <sub>2</sub> O)	0.03%
TiO <sub>2</sub>	Trace		

Temperature of Maximum Use---2173°K

Specific Gravity---3.80 (pure oxide, 3.97) gm/cm<sup>3</sup>

Apparent Porosity---0%

Modulus of Rupture---40,500 psi

Modulus of Elasticity--- $363 \times 10^{10}$  dynes/cm<sup>2</sup>

Specific Heat---0.27 cal/gm/°K (pure oxide)

Coefficient of Expansion<sup>15</sup>--- $5.9 \times 10^{-6}$  cm/cm/°K



TABLE IV

Characteristics of LA Series Ceramics<sup>14</sup>

<u>Mixture</u>	<u>Pore Size</u>
LA-830	10 microns $\pm$ 2
LA-831	25 microns $\pm$ 3
LA-832	40 microns $\pm$ 4

The resistance of the matrix-electrolyte combination is a function of the through pores only---those that are open on both ends. The equation

$$R = \frac{\rho \ell}{A} \quad (14)$$

describes the resistance of a conductor of resistivity  $\rho$ . In this case,  $\ell$  is the thickness of the matrix across the electrode area (ideal path length),  $A$  is the area of the available electrolyte, and  $R$  is the resistance in ohms. Electrolyte-matrix conductivity is the reciprocal of the resistivity,  $\rho$ . If no matrix were present,  $A$  would represent the full electrode area. However, since a matrix is interposed, the true value of  $A$  would be the combined area of the through pores that the two liquid metals contact. A means of determining the through pores, representing  $A$ , has been worked out in the Allison laboratories. This method involves measurement of the resistance of a cell containing a known area and thickness of one normal KCl solution whose conductivity is accurately known. A sample of matrix is then interposed after having been impregnated under vacuum with the same solution. The resistance is again measured by high frequency a-c methods. Thus, comparing the resistance measured with the matrix in place with the known resistance of the pure KCl solution, a ratio may be taken which is called the effective electrode area. This is representative of the pores open on both ends. The effective electrode area of the No. 5186 ceramic is 8-10 percent, and that for the LA series materials is as follows:



LA-830 21 percent  
 LA-831 23.6 percent  
 LA-832 21.7 percent

Thus, it can be seen that the use of the LA series matrices will yield conductivities two to three times higher than that for the No. 5186 matrix.

Electrolyte retention is based on the surface tensions of the electrolyte mixture held within the pores of the matrix and the surface tensions of the amalgams present in the cells. This can be strongly affected by the production of mercury vapor in the lower cell half, should overheating take place. A guide to the requisite pore sizes is available from mercury porosimeter tests which measure the pressures necessary to force mercury through unimpregnated or open pores. It must be remembered that the pressures necessary to force mercury vapors through an impregnated pore would be even higher.

$$p = - \frac{4\sigma \cos \theta}{D} = - \frac{175}{D} \text{ (Based on wetting angle, } \theta = 130^\circ, \text{ at room temperature)} \quad (15)$$

where  $\sigma$  is the surface tension of the liquid,  $\theta$  is the wetting angle,  $p$  is the applied pressure, and  $D$  is the diameter of the smallest pore filled at pressure  $p$ . From Equation (15), a pressure differential of 15 psi would cause mercury to pass through an empty pore approximately 15 microns in diameter. A pore of five-micron diameter would require a pressure of approximately 35 psi to force mercury into it.

The compressive strength of sintered alumina is considerably greater than its tensile strength.<sup>12</sup> At 673°K, the compressive strength is 15,000 kg/cm<sup>2</sup> while its tensile strength at 573°K is 2560 kg/cm<sup>2</sup>. The corresponding tensile strength of a heat treated steel is 4500 kg/cm<sup>2</sup> at 673°K.

### Reactants

The compilation of literature on amalgams is incomplete due to the dearth of literature on the subject.

A 90 percent (mole) potassium amalgam versus pure mercury in the cell (Figure 1) will give an open circuit emf of approximately 1.2 volts. Figure 3 indicates that as current is drawn, the depletion of potassium in the anode will lead to an increase in density of the anode amalgam, while the amalgam in the cathode will be decreasing in density as potassium is added to the raw mercury. Figure 4 is a plot of amalgam viscosity versus composition. Figure 5<sup>8</sup> shows that any place in the system where the mole percent of mercury is likely to approach 67 percent must be maintained at temperatures above 533°K to keep the system molten.

This condition could exist at the electrolyte-mercury interface where the mercury-rich amalgam would conceivably be formed.

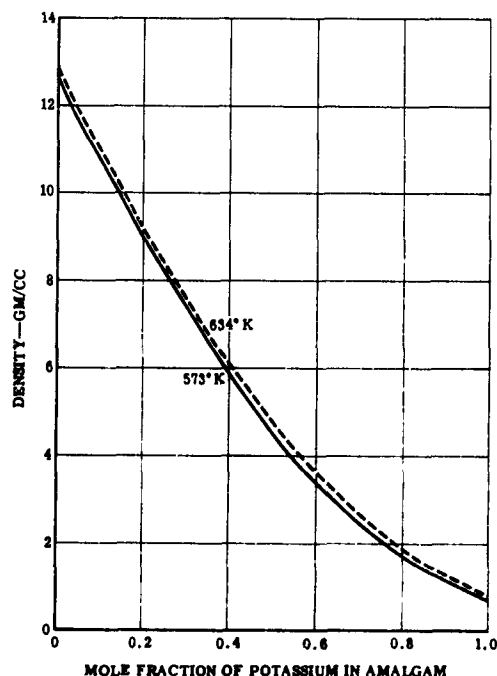


**Figure 3. Density of Amalgams as a Function of Composition**

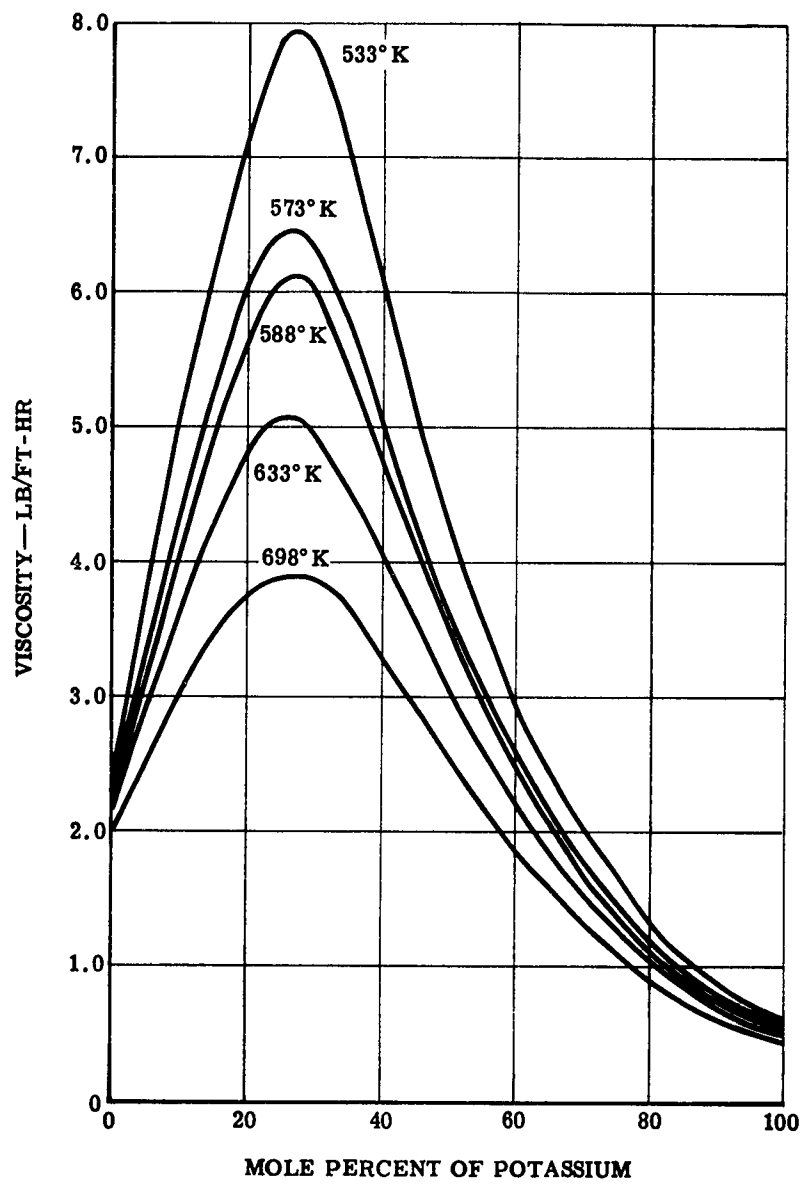


Figure 4. Amalgam Viscosity Versus Composition

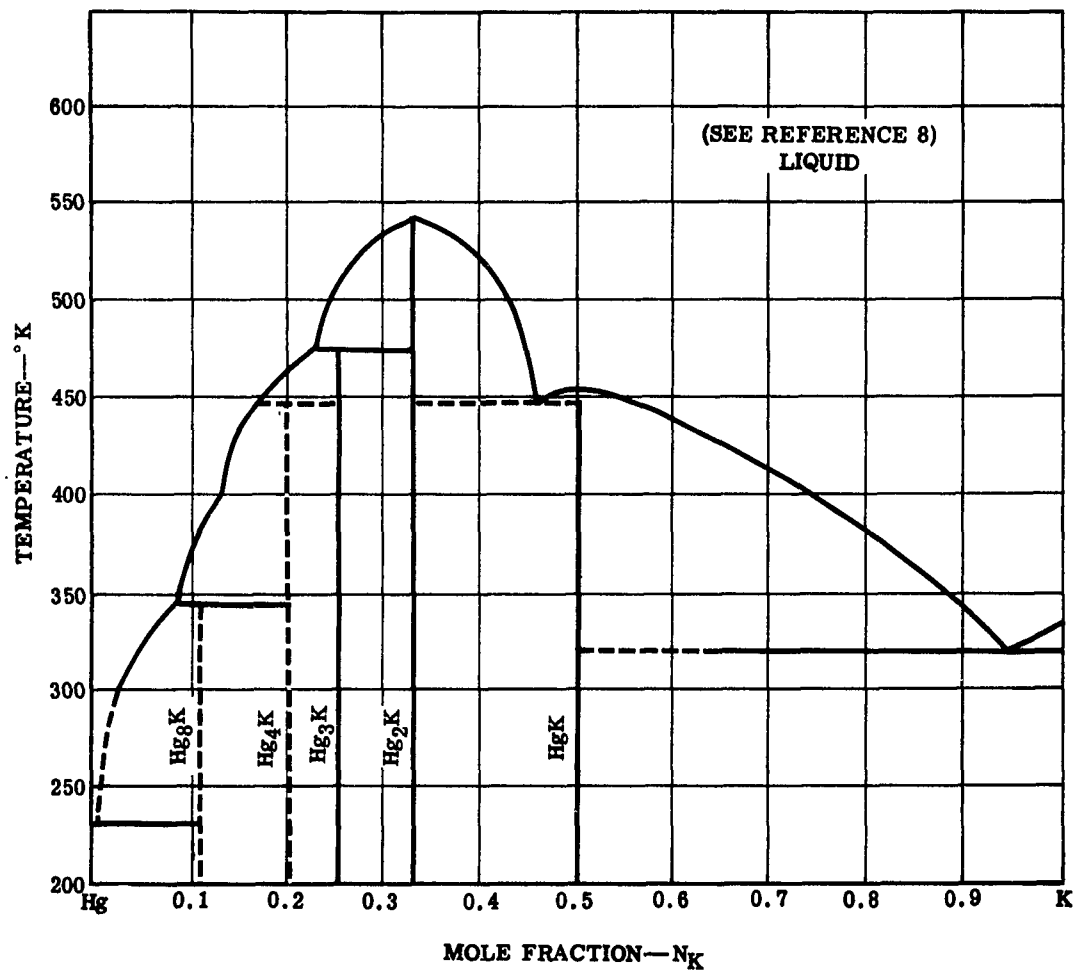


Figure 5. Phase Diagram of KOH System

The properties of mercury and potassium are listed in Tables V and VI.

TABLE V

Properties of Mercury Metal<sup>17</sup>

Melting Point—234.13°K

Latent Heat of Fusion—2.8 cal/gm

Boiling Point—630°K

Latent Heat of Vaporization—69.7 cal/gm

Density—12.881 gm/cm<sup>3</sup> (573°K)

Volume Change in Fusion—3.6% of solid

Vapor Pressure

<u>(mm Hg)</u>	<u>(°K)</u>
1	399.2
10	457.0
100	534.7
200	563.7
400	596.0

Heat Capacity

<u>(cal/gm/°K)</u>	<u>(°K)</u>
0.03334	273
0.03279	373
0.03245	473
0.03234	573
0.03256	723

Thermal Conductivity

<u>(cal/sec/cm/°K)</u>	<u>(°K)</u>
0.0196	273
0.0231	333
0.0261	393
0.0279	433
0.0303	493



TABLE V (cont)

Resistivity	
<u>(microhms)</u>	<u>(°K)</u>
98.4	323
103.2	373
114.2	473
127.5	573
135.5	623
Surface Tension	
<u>(dynes/cm)</u>	<u>(°K)</u>
465	293
454	385
436	473
405	573
394	627

TABLE VI

Properties of Metallic Potassium

Melting Point—336.7°K  
 Latent Heat of Fusion—14.6 cal/gm  
 Boiling Point—1033°K  
 Latent Heat of Vaporization—496 cal/gm  
 Vapor Pressure—1 mm Hg at 615°K  
 Density—0.783 at 523°K  
 Surface Tension—86 dynes/cm (373°-423°K)  
 Volume Change on Fusion—2.41% of solid  
 Heat Capacity

<u>(cal/gm/°K)</u>	<u>(°K)</u>
0.1956	348
0.1887	473
0.1826	673

TABLE VI (cont)

Viscosity	
<u>(centipoises)</u>	<u>(°K)</u>
0.515	342.6
0.331	440.4
0.258	523.0
0.191	673.0
Thermal Conductivity	
<u>(cal/sec/cm/°K)</u>	<u>(°K)</u>
0.1073	473
0.1013	573
0.0956	673
Resistivity	
<u>(microhms)</u>	<u>(°K)</u>
13.16	337
18.70	423
25.00	523
28.20	573
31.40	623
Solubility of Potassium in Fused Hydroxides <sup>19</sup>	
<u>(753°K)</u>	<u>(873°K)</u>
7.8-8.9 gm/100 gm	3-4 gm/100 gm
<u>(923°K)</u>	<u>(973°K)</u>
2-2.7 gm/100 gm	0.5-1.3 gm/100 gm

Handling metallic potassium with the intent of maintaining any degree of purity is a difficult and tedious procedure. Not only is potassium highly reactive with moisture or air, but it is exceedingly difficult to procure potassium which does not have dissolved oxides. Various techniques are reported<sup>18</sup> for the purification of potassium using a titanium or zirconium sponge. These techniques do not work well in an amalgam since both titanium and zirconium

show some solubility in the mercury and their effect on the system is unknown at this time. The reaction of potassium with water is well known by nature of its violence. In the presence of a minute amount of oxygen, a clean potassium surface will quickly cloud over with oxide and, under the proper conditions, may form an explosive peroxide.

### Electrolyte

The electrolyte is a molten salt mixture containing potassium as the common cation. This electrolyte was chosen mainly on the criteria of proper melting point; lack of reaction with the liquid metals, matrix, or container; the absence of thermal decomposition; and good electrical conductivity. Three electrolyte systems are being considered—two are binary systems and one is a ternary system. The binary systems consist of (1) potassium hydroxide-potassium bromide, which shows a eutectic of 573°K at a composition of 65 percent (mole) potassium hydroxide; and (2) a mixture of potassium hydroxide-potassium iodide, which shows a eutectic of 523°K at a composition of 72 percent (mole) potassium hydroxide. The ternary system, KOH-KBr-KI, has been surveyed in the Allison laboratory. The exact eutectic composition has not been determined, but indications are that the eutectic temperature will be between 493° and 503°K. Phase diagrams<sup>20</sup> of the binary systems are shown in Figures 6 and 7. A three-dimensional model of the ternary system is shown in Figure 8.

The allowable melting point range of the electrolyte system is limited by the minimum temperature as determined from the potassium-mercury phase diagram (Figure 5) at 553°K, while the upper end of the melting point range must not exceed the boiling point of mercury.

All three of the systems mentioned fall within these requirements—the potassium hydroxide-potassium bromide system is the highest melting system, and the ternary (potassium hydroxide-potassium bromide-potassium iodide) system is the lowest melting system. Selection of an electrolyte system would then be based on the following considerations:



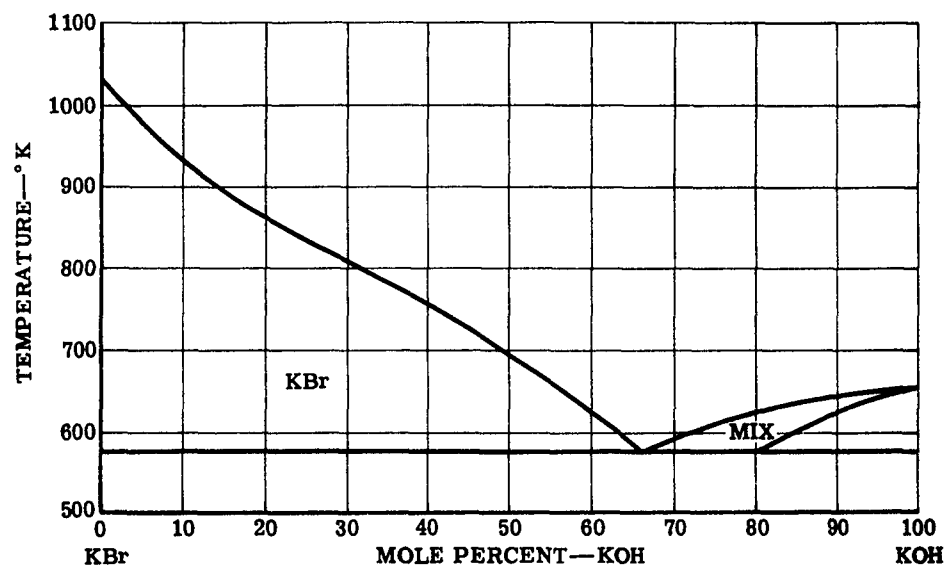


Figure 6. Phase Diagram of KOH-KBr System

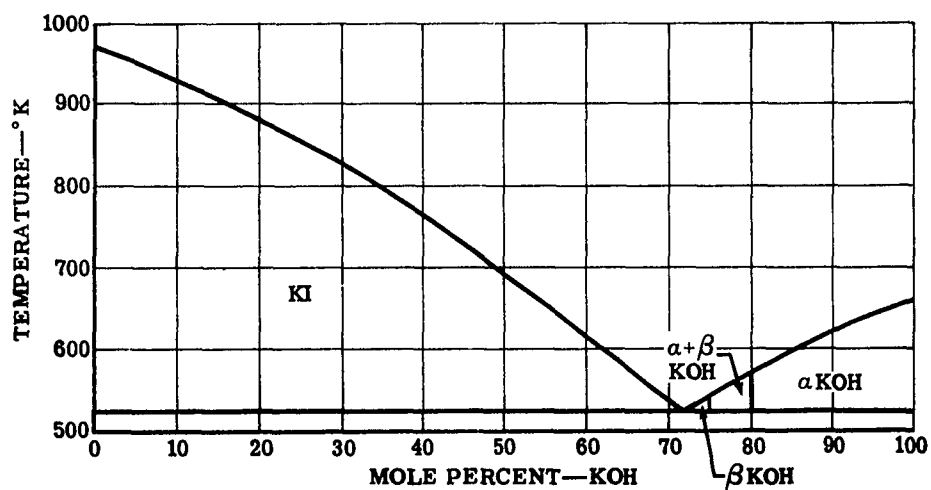
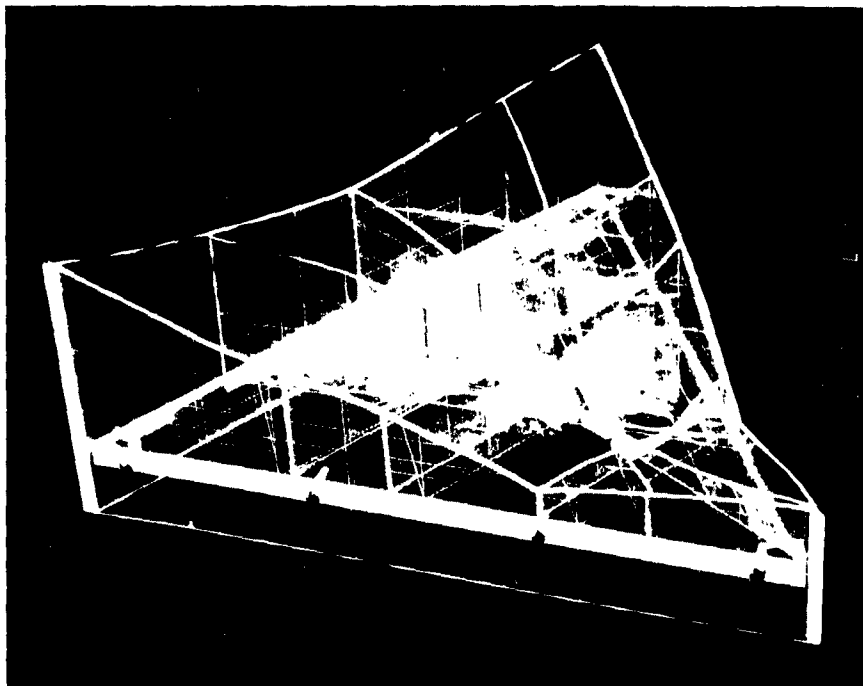


Figure 7. Phase Diagram of KOH-KI System



**Figure 8. Phase Model of KOH-KBr-KI System**

1. The further the cell operating temperature from the melting point of the electrolyte, the better the conductivities expected.
2. The further the melting point of the electrolyte system from the boiling point of mercury, the less danger of overheating due to heat generated within the cell.
3. The lower the percentage of potassium hydroxide in the system, the less corrosion there should be on the ceramic parts.

The ternary system fits these qualifications best and is therefore the one in use at the present time. The noneutectic mixture of 60 percent (mole) potassium hydroxide-20 percent (mole) potassium bromide-20 percent (mole) potassium iodide is being used. This electrolyte has a resistivity of approximately 1 ohm-cm ( $\rho$ ) and contains less potassium hydroxide than either of the other two systems. Compatibilities of this system with the proposed ceramic materials has been determined and found to be successful for periods of 336 hours. Tests on reagent grade potassium hydroxide have shown that dewatering of this hygroscopic material at 623°K in an argon inerted atmosphere evolved an average of 11.5 percent water, while a vacuum treatment at the same temperature evolved 17.3 percent water. Since water has been found to be detrimental to the life of the ceramics, it is important in the preparation of any electrolyte system that it be adequately dewatered under vacuum.

## CONSTRUCTION

### Laboratory Cells

Two approaches to the basic cell design are being considered for this program. The first approach consists of a circular cell which would utilize a matrix of approximately 46-cm<sup>2</sup> electrode area. To bypass the problems involved in differential thermal expansion between the ceramic matrix and the metallic body of the cell, and the problems associated with the differential head of pressure in the lower chamber, the floating concept can be used in the circular cell. This concept utilizes a compression seal of the cell along the outer rim of the basic circle, the compression being applied from the upper to the lower half. A dense A-402 alumina gasket is used on the upper rim to electrically insulate the two halves. The ceramic matrix is approximately 0.01 cm undersized in thickness. The difference allows this capillary passage to fill with molten electrolyte. When mercury is run into the lower chamber, the matrix will float on top of the mercury and will act



as a check valve between the upper and lower chambers. Therefore, the mercury or amalgam will not be able to travel between chambers. At the same time, the matrix is free to expand and to move about as conditions demand. The pressure heads associated with this cell are very closely controlled through the location of the feed pot, the collection pot, and the piping coming to and from the cell. An alternative to the floating matrix, which could be incorporated in this cell, would be a normal seal in which the matrix would bear the compression between halves of the cell and serve as part of the compression seal. An O-ring would then seal against the dense gasket of the upper cell half and against the metal rim of the lower cell half.

The second approach to the construction of the basic cell would involve an attempt to increase its size so that fewer assemblies will be needed in the 310-watt stack. It should be mentioned that as each new step is made throughout the program to develop larger matrices, time and problems involved will be increased. It should be remembered that the rectangular cell is an alternate approach—it is an "island hopping" technique whereby the possibility may exist of using a larger cell than the one originally considered feasible. The rectangular cell being considered consists of a porous piece of ceramic enclosed on four sides by a dense impervious ceramic frame. The porous portion would be approximately 0.3 cm thick and the A-402 impervious frame would be approximately 0.9 cm thick. The over-all cell area would be 232 cm<sup>2</sup>. If practical, the floating concept could be incorporated in this frame to simplify the construction of a cell or a stack of cells of this type.

Feed and effluent piping would consist of holes drilled through the metal plates which form the barriers between cells when compressed to either side of the frame. At the same time, the plates would act as the series electrical connection from one cell unit to the next. In this fashion the cell stack can be built up to any given voltage. A view of the bottom half of the circular cell is shown in Figure 9. The outer rim is used for the compression seal of the floating-type cell, or to hold the O-ring groove for the matrix-type seal; the next lower plateau holds a circular matrix and the electrolyte replenishment annulus; and the lowest level is the mercury chamber.



**Figure 9. Bottom Half of Circular Cell**

Figure 10 is a typical view of the No. 5186 matrix and the A-402 impervious gasket used in the cell. Figure 11 is a view of the top half of the cell showing white faces which have been flame sprayed with aluminum oxide (originally considered as an insulating material), but the flame sprayed alumina has not been used in later cells because of its poor compatibility with the amalgam and the electrolyte. Figure 12 shows the two cell halves as they would be assembled in the press. Figure 13 shows the experimental setup for running either rectangular or circular cells. Detail drawings of these cell halves are shown in Figures 14, 15, and 16. In the view of the bottom side of the cell, tubes 13, 2, and 7 will have electrical sensors (Figure 17) attached to them to indicate (1) the levelness of the cell, (2) the point at which the mercury level just reaches the matrix, and (3) the point at which the mercury head is sufficient so that a possible breaching of the seal might take place. Tubes 1 and 3 will feed out approximately an 8 percent (mole)

potassium amalgam under a 10-amp load and a mercury feed rate (at room temperature) of 1 cm<sup>3</sup>/min. Pure mercury will feed through either tube No. 4 or bypass tube No. 6; tube No. 7 is a drain for the mercury side of the cell; and tube No. 5 will allow electrolyte to seep into the electrolyte annulus to replenish any possible electrolyte losses. The thermocouple well is indicated as extending into the interior of the cell.

With reference to Figure 15, the amalgam side of the circular cell, tube No. 8 is an argon inlet which will allow argon to sweep through the upper half of the cell and clear it of air before and after loading the cell; tubes No. 9 and 11 allow either 90 percent potassium amalgam or pure potassium to flow into the upper cell half; tube No. 10 could be used to drain the cell if it is desired to change amalgam composition or to shut down the cell for disassembly; tubes No. 12 and 14 are overflows for the potassium side. Figure 16 is a drawing of the proposed intermediate cell (exclusive of piping) to be used in the construction of a basic cell unit. The intermediate cell is merely a combination of a bottom half and a top half built in one piece for a series connection—all piping being as indicated in Figures 14 and 15.



**Figure 10. No. 5186 Matrix and A-402 Gasket**

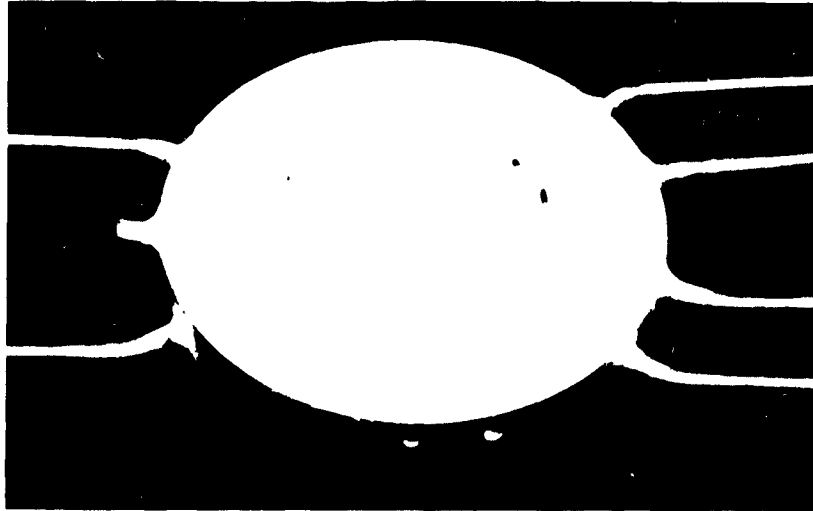


**Figure 11. Top Half of Circular Cell**

Figure 18 shows a rectangular cell with a wooden simulated picture frame matrix in place. Figure 19 shows the cell as it would actually look, exclusive of the cell press. A detail drawing of the assembled cell is shown in Figure 20. It should be noted that from each pair of adjacent pipes, one feeds down to the chamber below the plate while the other feeds up to the chamber above the plate. Thus, each plate can be considered as an intermediate type. The feed system was tested at ambient temperatures using mercury in both cell chambers of the simulated picture frame. Construction of both the circular and rectangular cells is of 410 stainless steel. Figure 21 is a photograph of a preliminary three-cell stack shown assembled in its press. Details of the cell press are shown in Figures 22 through 27.

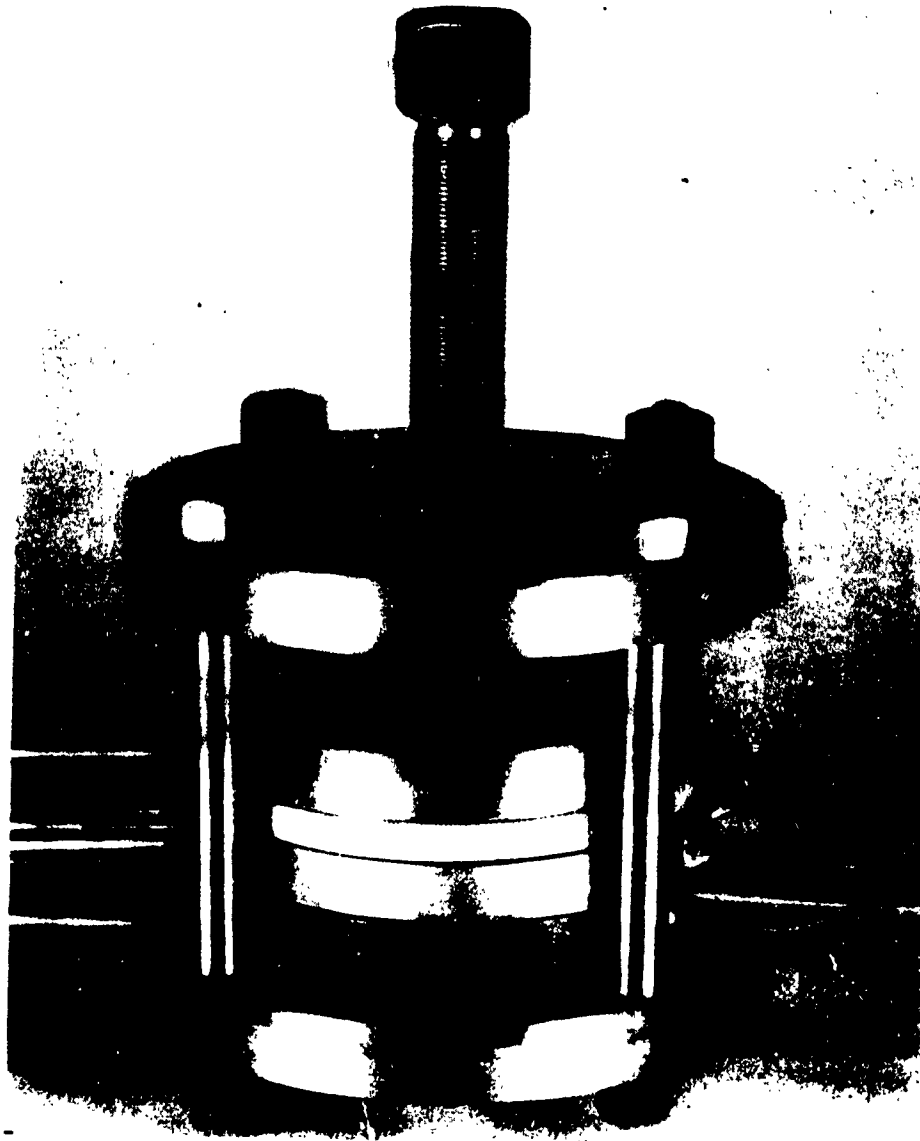


Figure 12. Cell in Press



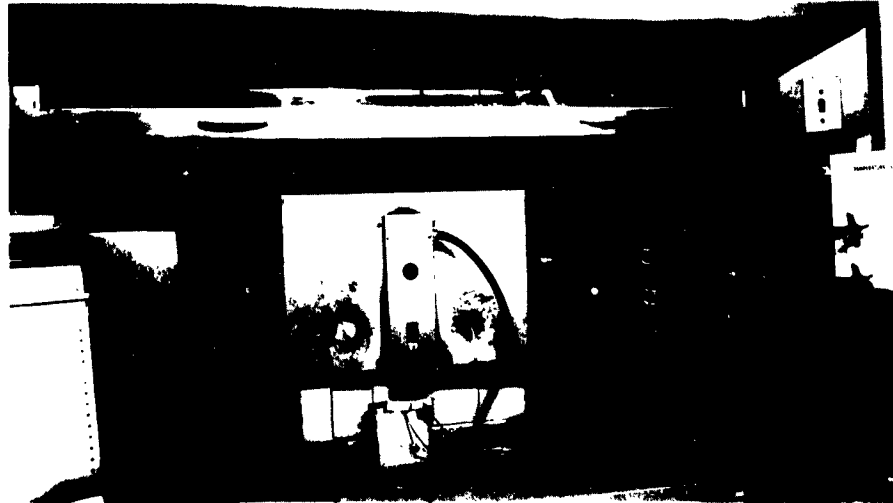
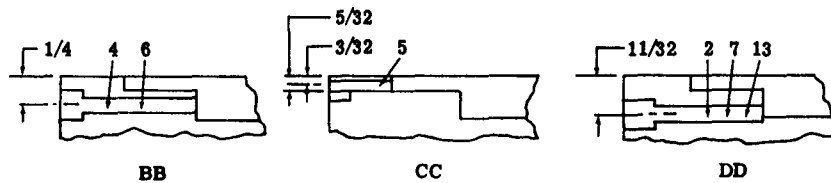
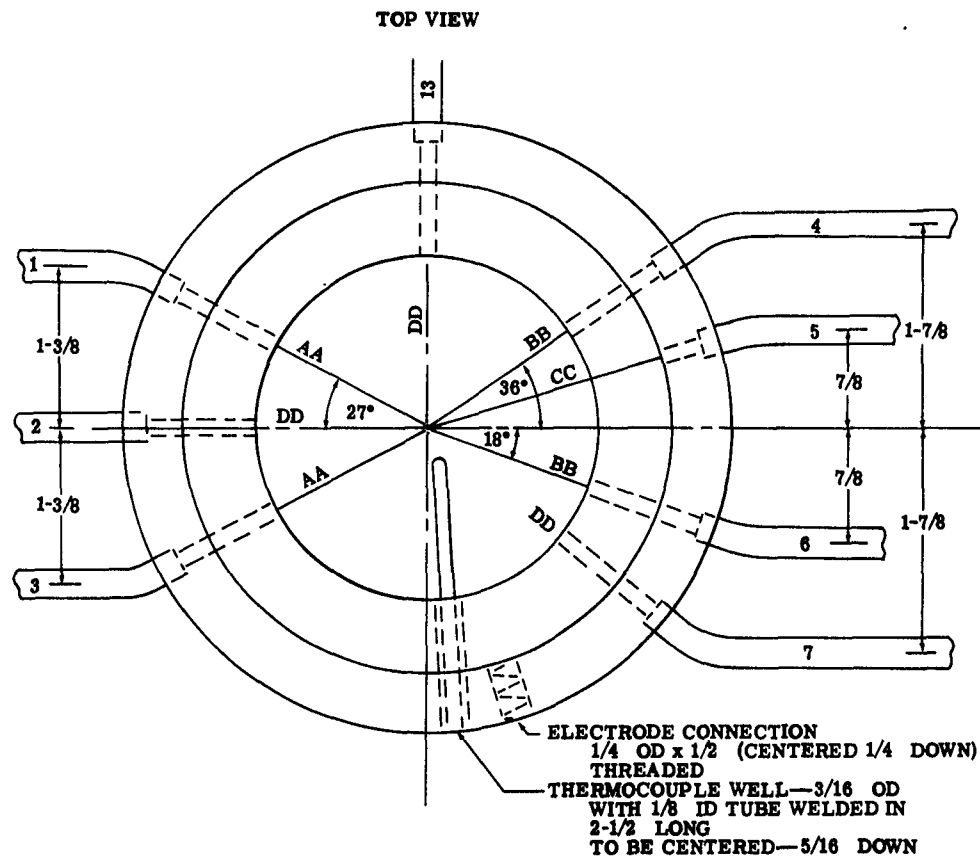


Figure 13. Experimental Setup



ALISON



ALL HOLES—1/8 AND ALL TUBES—1/4 OD  
UNLESS OTHERWISE NOTED  
ALL HORIZONTAL SURFACES TO BE GROUND  
PARALLEL AND FLAT TO  $\pm 0.0005$  IN.

Figure 14. Detail of Bottom Half of Circular Cell

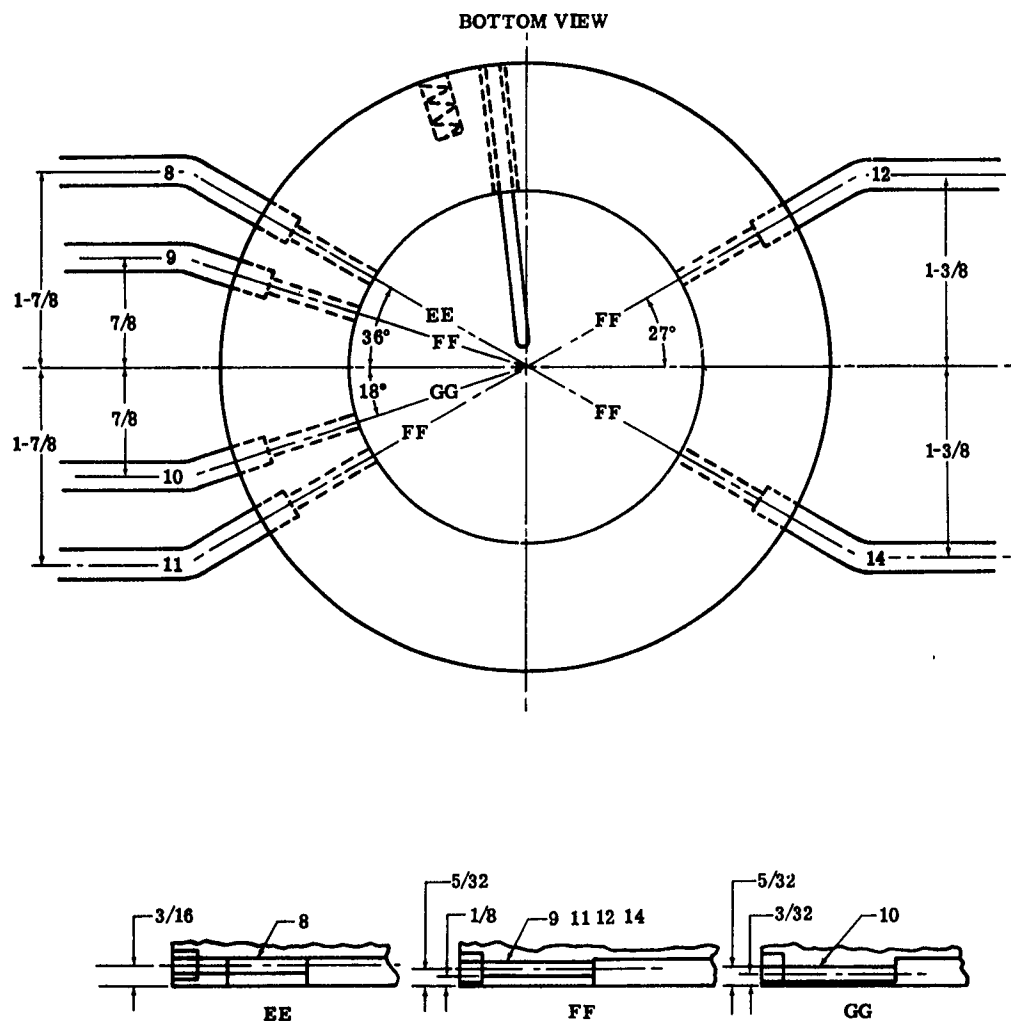
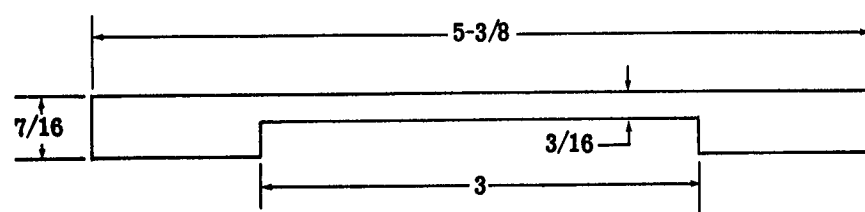


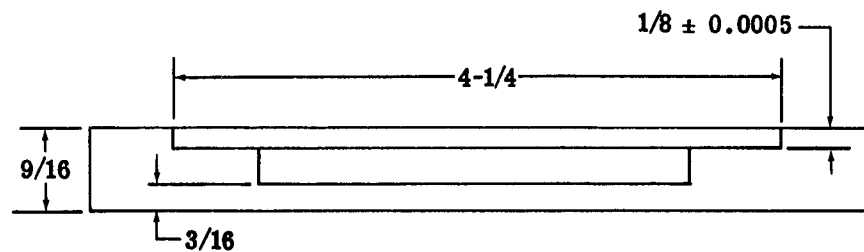
Figure 15. Detail of Top Half of Circular Cell

### TOP CELL



(ALL HOLES TO CORRESPOND TO BOTTOM  
VIEW OF INTERMEDIATE CELL)

### BOTTOM CELL



(ALL HOLES TO CORRESPOND TO TOP  
VIEW OF INTERMEDIATE CELL)

### SECTION AA

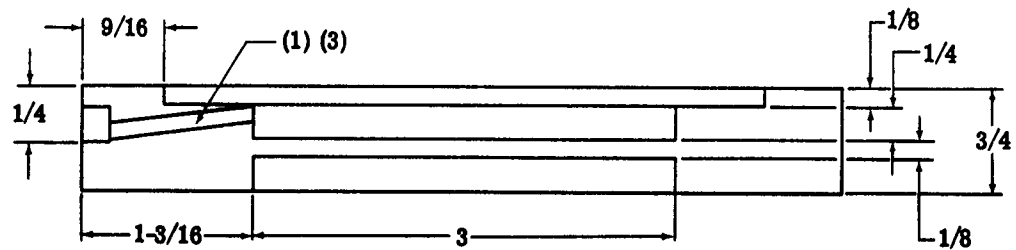


Figure 16. Detail of Cell Profile and Intermediate Type Cells



Figure 17. Level Sensor

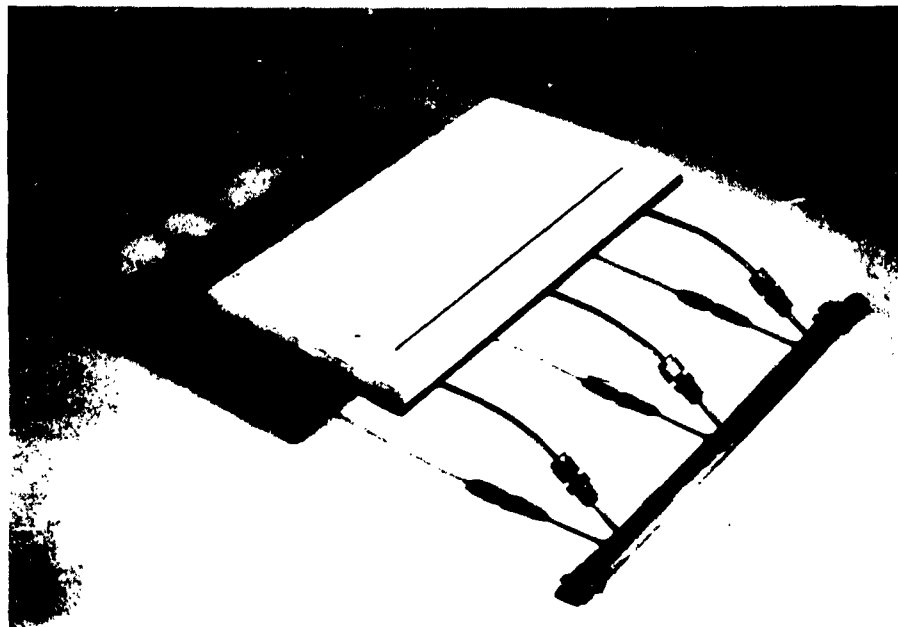


Figure 18. Rectangular Cell with Matrix in Place



**Figure 19. Rectangular Cell Outside of Press**

Operation of the feed systems for single cells has been very simple and consists merely of an open feed pot for the mercury, whose level can be adjusted by raising or lowering a laboratory jack. In this manner the hydrostatic head of the mercury feeding through the cell half can be controlled. A large pot is located near the exit tubes outside the furnace for collection of the mercury effluent. Figure 28 is an inerted pressure feed pot for the amalgam side of the cell. To date, a stainless steel pot was used for electrolyte replenishment, but this will be replaced by a ceramic pot contained within the furnace unit since the ceramic does not indicate any breakdown, as does the stainless steel.

Instrumentation to date has been kept simple—a multichannel recorder is used for measuring temperatures of (1) upper and lower cell halves, (2) the mercury feed, (3) the amalgam feed, (4) the effluent, and (5) the electrolyte feed pot.

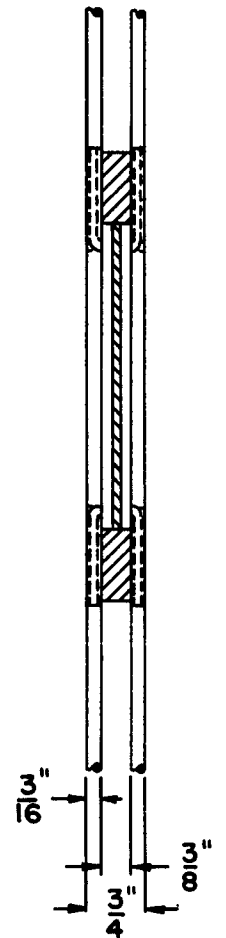
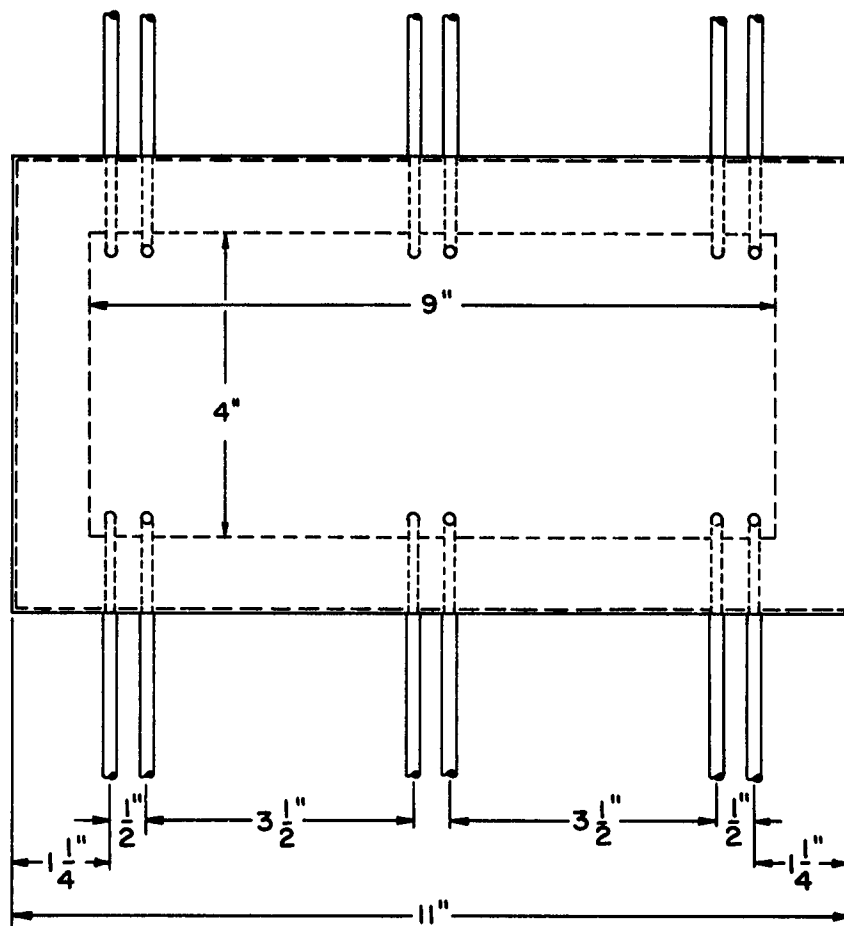


Figure 20. Detail of Rectangular Cell

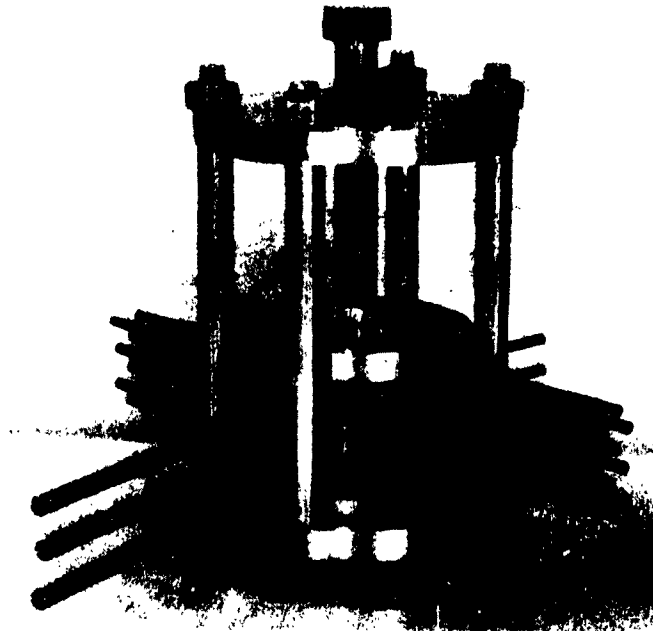


Figure 21. Cell Stack

The furnace is an inverted Norman kiln which is controlled through a Pyro-vane controller and can be raised or lowered for the experimental setup by a frame and two jacks.

The impregnation tank (Figure 29) is contained within another Norman kiln and is constructed of stainless steel of dimensions capable of handling either small ceramics or the large picture frames. Based on experience gained from the compatibility tests, the impregnation procedure is as follows:

1. The electrolyte is mixed in proper proportions and held under vacuum at 623°K for two days.



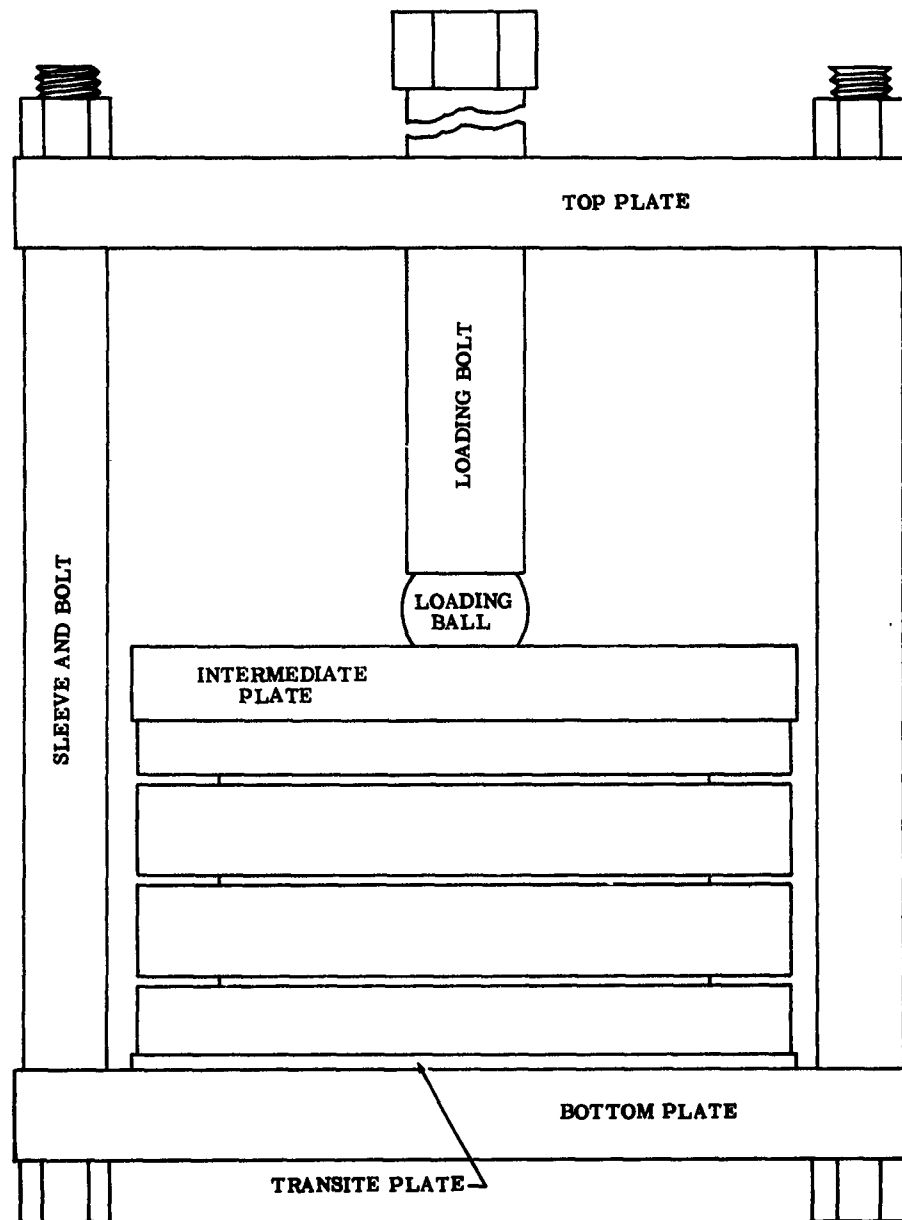
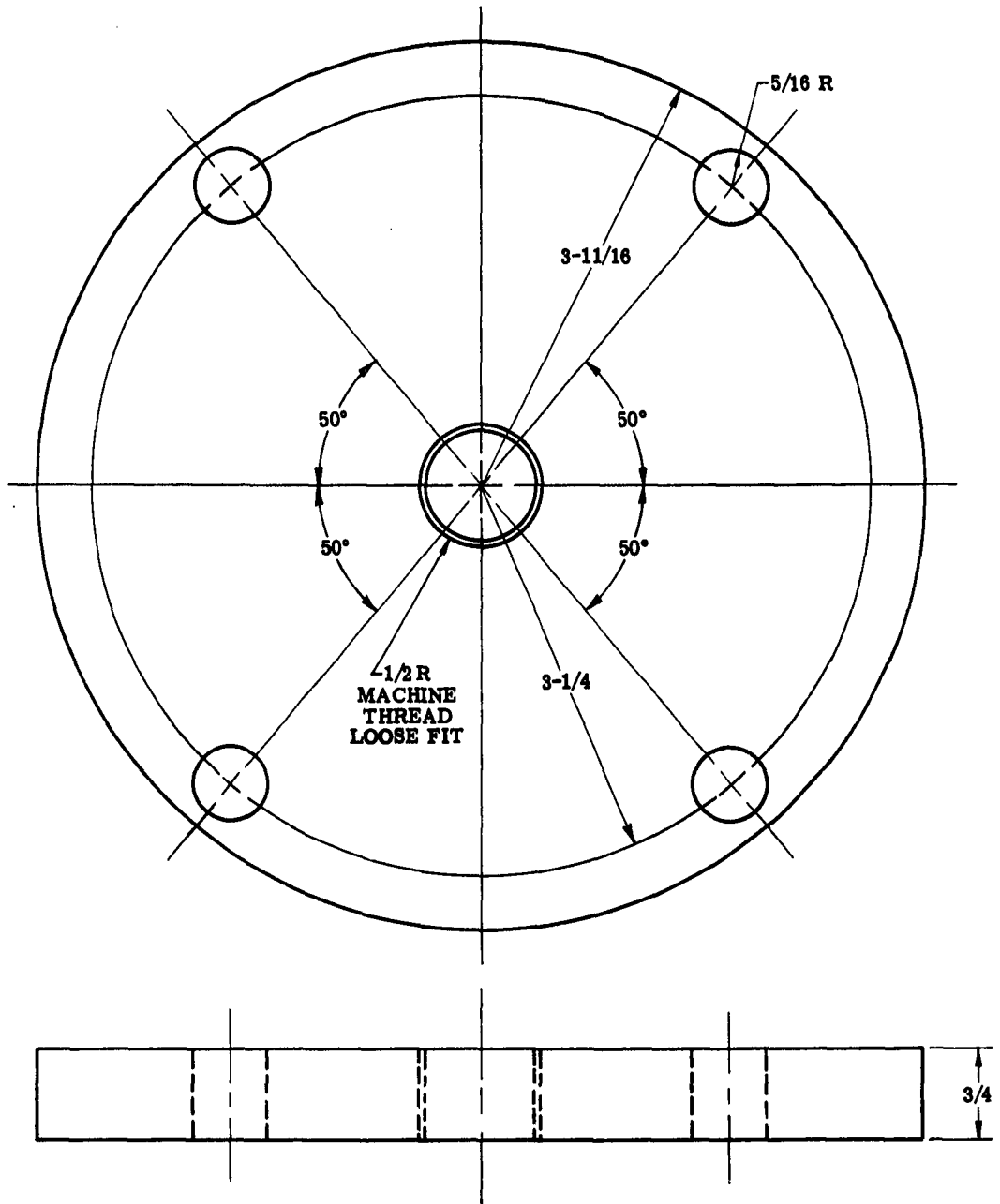


Figure 22. Press Assembled



**Figure 23. Press—Top Plate**

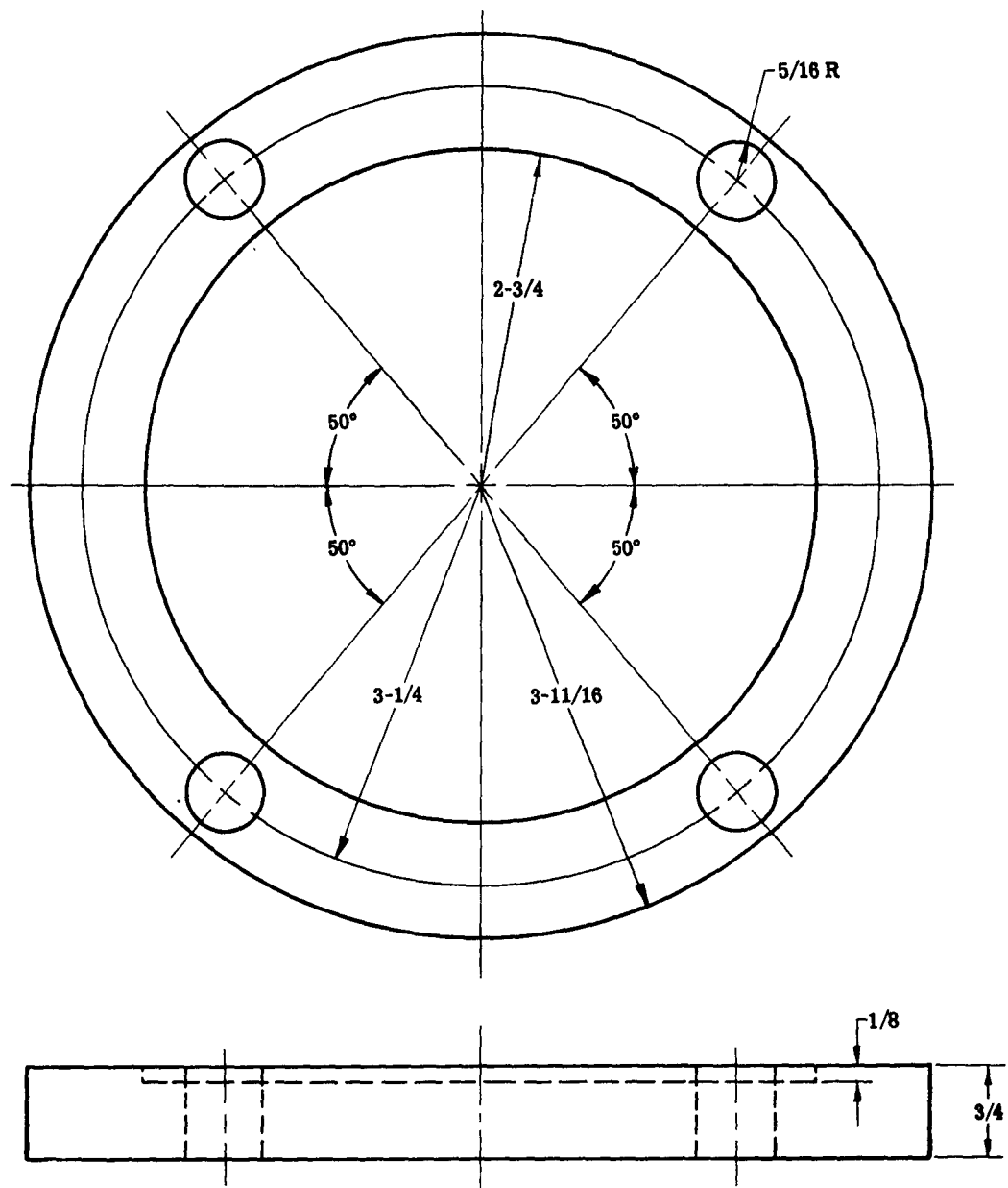


Figure 24. Press—Bottom Plate

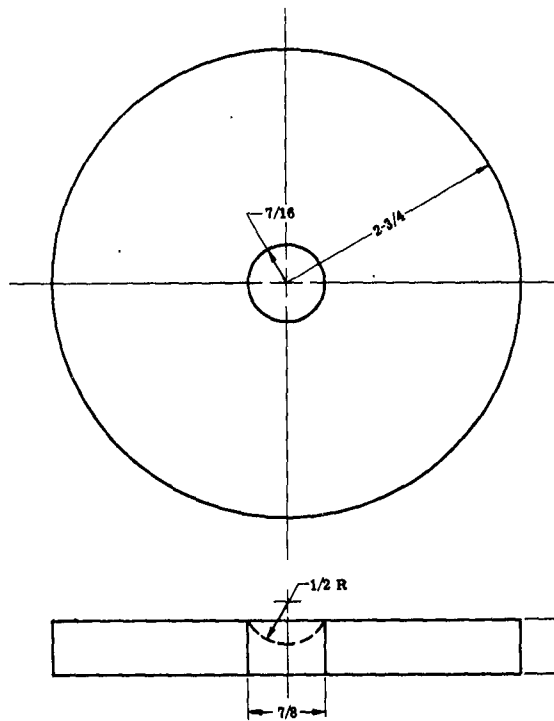
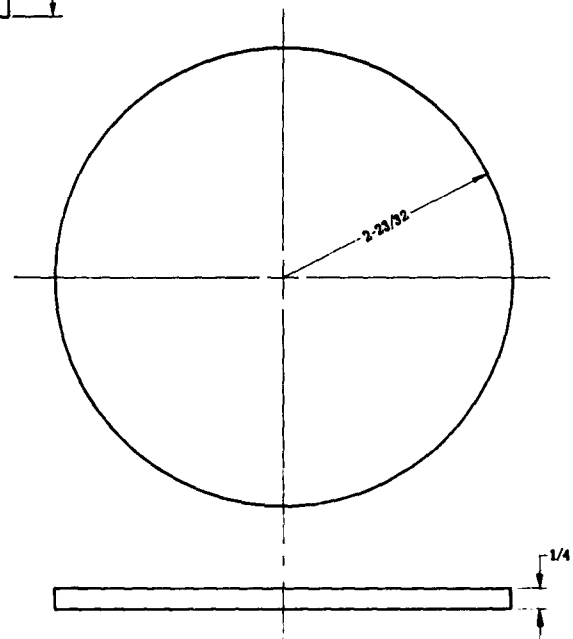


Figure 25. Press—Intermediate

Figure 26. Press—Transite  
Insulating Plate



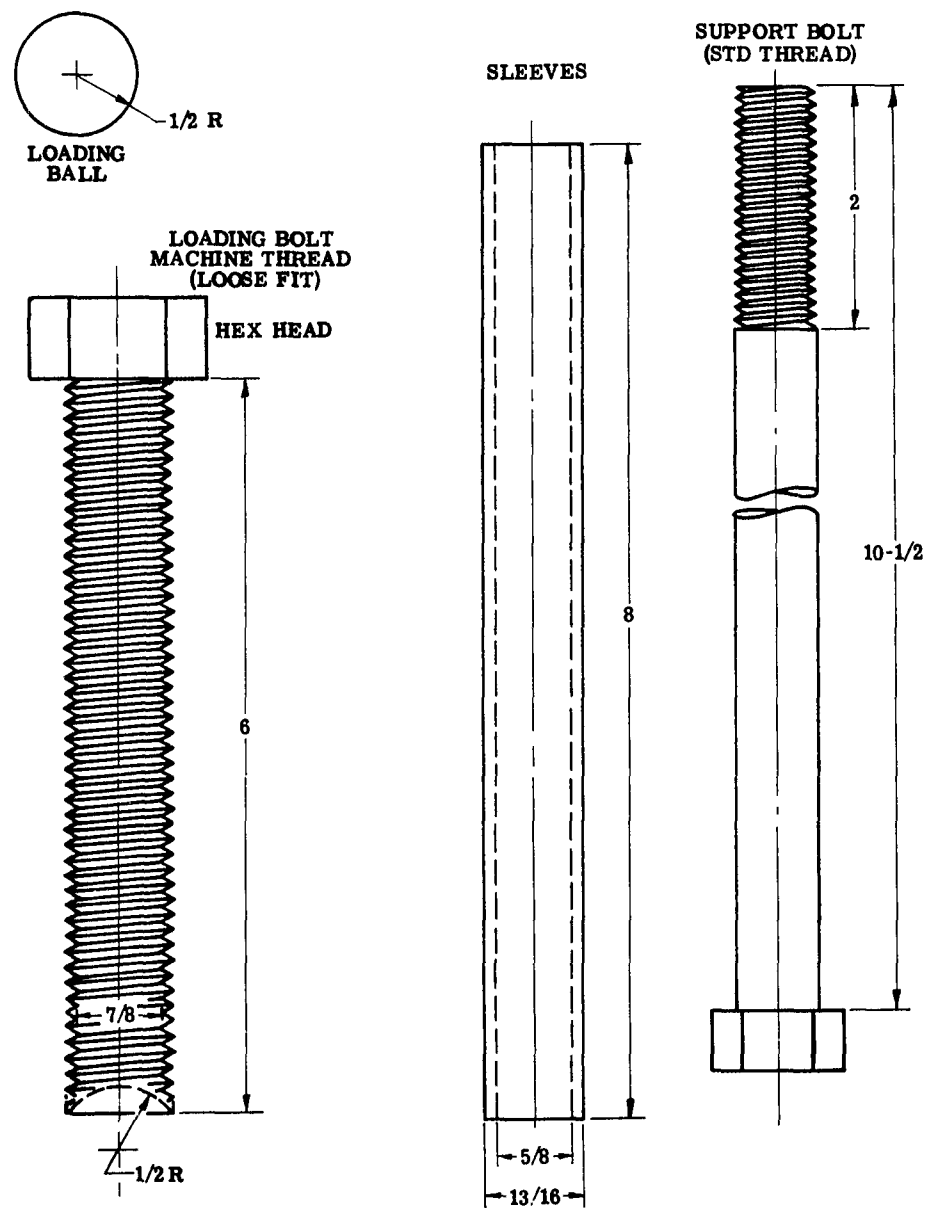


Figure 27. Press—Small Parts

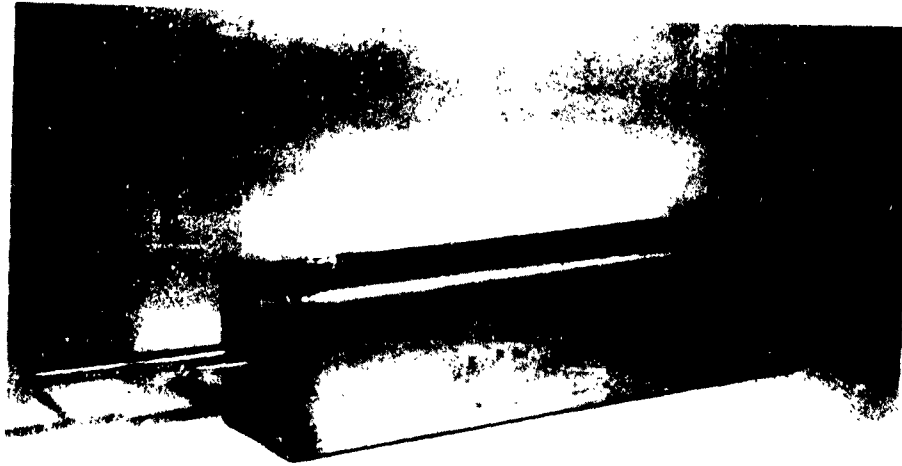


Figure 28. Feed Pot

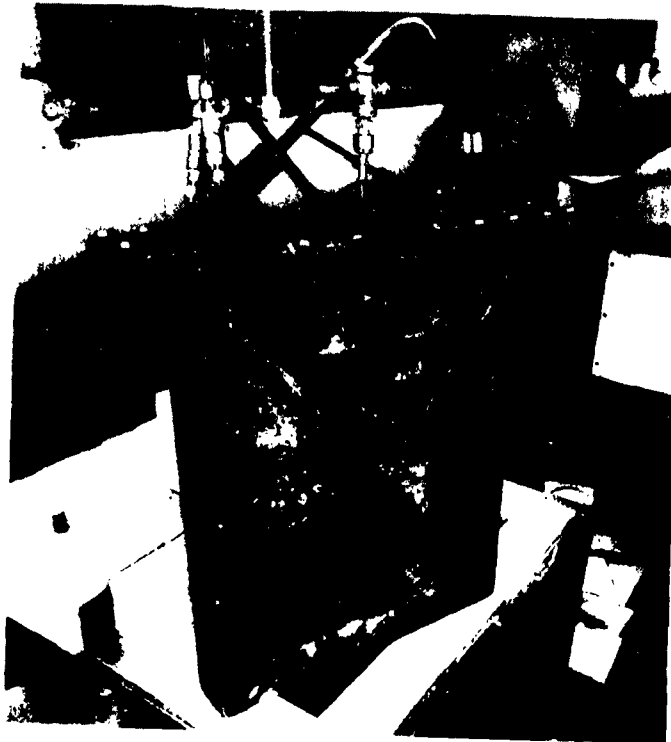
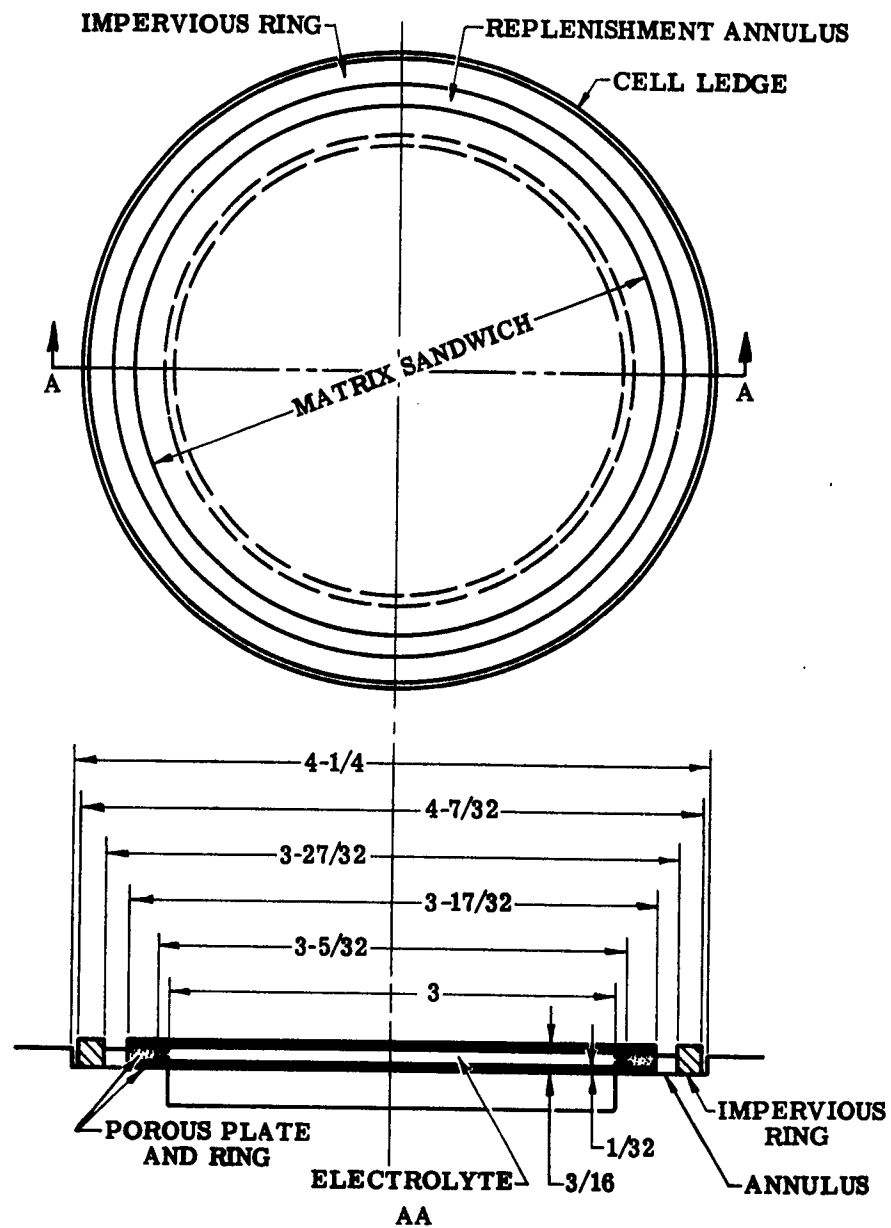


Figure 29. Impregnation Tank

- 
2. Samples are placed in a basket held above the electrolyte level, the tank is sealed, and a vacuum of 200 microns is drawn overnight which further dewateres the electrolyte and the oven-dried ceramic specimens.
  3. Following deaeration, the basket and samples are dipped below the surface of the electrolyte by use of a plunger passing through the tank cover---they are held in this position for 15 minutes.
  4. Vacuum is broken by addition of high purity argon and a pressurization cycle takes place.
  5. Items 3 and 4 are repeated for four cycles, whereupon the plunger, basket, and samples are raised and readied for use.

Several types of matrix design are under consideration. One utilizes a flat circular disc, another has the center portion ( $46 \text{ cm}^2$ ) dished out to a thickness of 1.25 mm, and another type (Figure 30) is a sandwich construction which is 0.48 cm thick. However, by nature of its construction, the expected matrix resistance would be comparable to that of a solid matrix of 2.5-mm thickness. Finally, the picture frame matrix (Figures 18 and 20) comprises the last of the proposed matrix types.



**Figure 30. Matrix Design**



## IV. EXPERIMENTAL RESULTS

### PRELIMINARY TESTS

The circular cell was tested at ambient temperature using mercury in both the upper and lower chambers and with water simulating the molten electrolyte. Tests of this nature on the floating seal did not produce a leak during extensive trial running of the system. A similar test was run on the completed rectangular cell using the wooden simulated picture frame matrix and this, too, produced no leaks. Testing of the rectangular cell at cell operating temperatures (573-623°K) has been held up by delay in the delivery of the completed ceramic picture frames from the manufacturer.

### STABILITY TESTS

Three circular cells were assembled and tested at an operating temperature of 598°K to determine the voltage stability of the cell design. Instability would indicate leakage between cell halves or possible reactions taking place as was indicated under the discussion of the electrolyte and amalgams. The first cell tested was of the floating matrix type. The cell was heated and charged, and during its early hours of operation there were no indications of instability. Using a 90 percent (mole) potassium amalgam versus pure mercury, the cell developed an emf of 1.1 volts, but after several hours of operation, a self-discharging mode was indicated in which the cell voltage started to fall off gradually. Upon standing over night, the emf had dropped to 0.2 volt. Flushing the lower chamber with fresh mercury and recharging the upper compartment with fresh amalgam restored the open circuit voltage to approximately 0.6 volt. Within a short time thereafter, the cell leaked and completely shorted. Examination of the cell indicated that the flame-sprayed alumina (which had been used at that time for insulation) had been grossly attacked by the electrolyte, exposing the underlying metal and allowing the matrix more than the specified 0.01-cm movement. This condition has now been corrected with a gasket of the A-402 impervious alumina with proved durability in molten electrolytes.

The other two cells assembled were used to test the compression-type seal using matrices of 0.48 cm and 0.64 cm. In these cases the external seal was on the matrix with no contact between the cell rims. The second cell, when loaded with a 90 percent (mole) potassium amalgam, established a stable emf of 1.2 volts but failed on the second day when an exit tube clogged and the seal was breached. A third cell with a 0.64-cm matrix resulted in low power output. Voltage stability was good, but the cell indicated a high initial internal resistance.

#### POWER OUTPUT TESTS

The resistance of the 0.64-cm cell, initially 3.1 ohms, later increased to the 30-ohm range, and still later dropped to 12 ohms. Just before failure, the resistance again increased to the 30-ohm range. A cell using a No. 5186 matrix of these dimensions (assuming an effective electrode area of 8-10 percent) should yield a matrix resistance of about 0.14 ohms, plus contact on other internal resistances. When disassembled and examined, the cell matrix showed areas through the cross section that were filled with a gray, metallic appearing material (Figure 31). Microscopic examination indicated that this gray material consisted of potassium-mercury amalgam. The maximum power output of the cell was 0.03 watt.

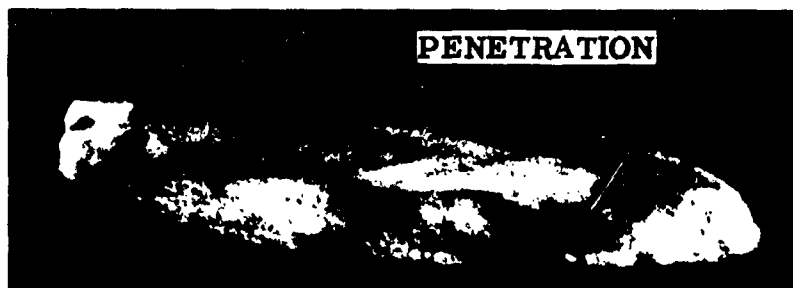


**Figure 31. Shorted Matrix**

Another cell of the new matrix configuration was then assembled using the No. 5186 material. This matrix had a thickness of 0.48 cm around the rim, but the thickness of the area separating the electrode compartments was 0.15 cm. This cell was put into operation immediately after the installation of the vacuum impregnated matrix. With an open circuit voltage of 0.98 volt, 3 amperes were delivered for a short time at a cell voltage of 0.52 volt for a power output of nearly 1.6 watts using a 90 percent (mole) potassium amalgam versus pure mercury. These conditions yielded almost maximum power density. The seal was breached at this point and, by the time the cell press was tightened down to eliminate the leak, a tenfold change in cell resistance from the initial 0.153 ohm took place. The cell continued to operate at low power densities for the next four days. On the fifth day, a higher power output of approximately 0.35 watt was obtained, and on the sixth day the cell shorted out. Disassembly of the cell and examination of the matrix again showed potassium-mercury amalgam permeating the cross section of the matrix. The calculated matrix resistance for a cell of this type should be 0.03 ohm. As indicated previously, the cell resistance (matrix resistance plus any contact resistance or IR drops from cell to the voltage take-off leads) was calculated as 0.153 ohm during the early stages of operation, 1.5 ohms during the middle stages, and 1.2 ohms just before failure.

It is felt that the change in resistance exhibited by the two foregoing cells is due to electrolyte depletion, as a result of the fact that these matrices were not sealed off from contact with outside atmosphere. The new matrix design (Figure 30) has been prepared to overcome this deficiency and should prevent shorting through the pore sections of the matrix. Shorting due to capillary replacement of the electrolyte by the mercury or sodium will be eliminated because there is no capillary path for the liquid metals to follow. Electrolyte replenishment will take place through the replenishment annulus which will be enclosed when the O-ring is added to the seal design.

The feed system functioned well for purposes of this experiment. A few minor improvements were indicated through the operation of these first cells, and these changes are being made.

## V. PRELIMINARY DESIGN OF A MULTICELL STACK

Preliminary design work has been initiated on a 310 watt stack of circular type cells utilizing matrices of 46-cm<sup>2</sup> area. With improvements in matrix design and material it is not unreasonable to plan for 10 amp/cell at an operating voltage of 0.5 volt. This would lead to an arrangement as shown schematically in Figure 32, which is a top view of the cell stack as it would look enclosed in the oven. Using a 6.35-cm thick fire brick for furnace construction, the projected furnace size in the preliminary plan would be 96.5 cm wide, 42.3 cm deep, and 74.7 cm high. It should be emphasized that no great consideration was given to weight, compactness, or complexity in this design. The stack is designed primarily with the philosophy that any needed adjustments or repairs can be made without a complete shutdown, and that the instrumentation necessary to fully evaluate the operating characteristics of the cells and stack should be included. Future cell stacks will be more compact, lighter, and use less tubing than indicated in the preliminary design. The nomenclature in Figure 32 is identified as follows.

- No. 1 indicates the top view of the press which holds three units of seven cells each, or a total of 21 cells.
- No. 2 is an inerted collector-interrupter for the amalgam overflow from the anode compartment. It is planned that as potassium is drawn electrochemically to the cathode chamber, it will be replaced in the anode of the cell by periodic injections of pure potassium from the potassium feed rather than maintaining a steady flow of amalgam through the upper cell half. This will permit a more thoroughly cleaned and purified potassium feed—low in K<sub>2</sub>O impurity.
- No. 3 indicates the mercury weirs to be fed from a large mercury feed pot. A detail drawing of the mercury weirs is shown in Figure 33. These weirs are also shown in Figure 34, which is a schematic of the

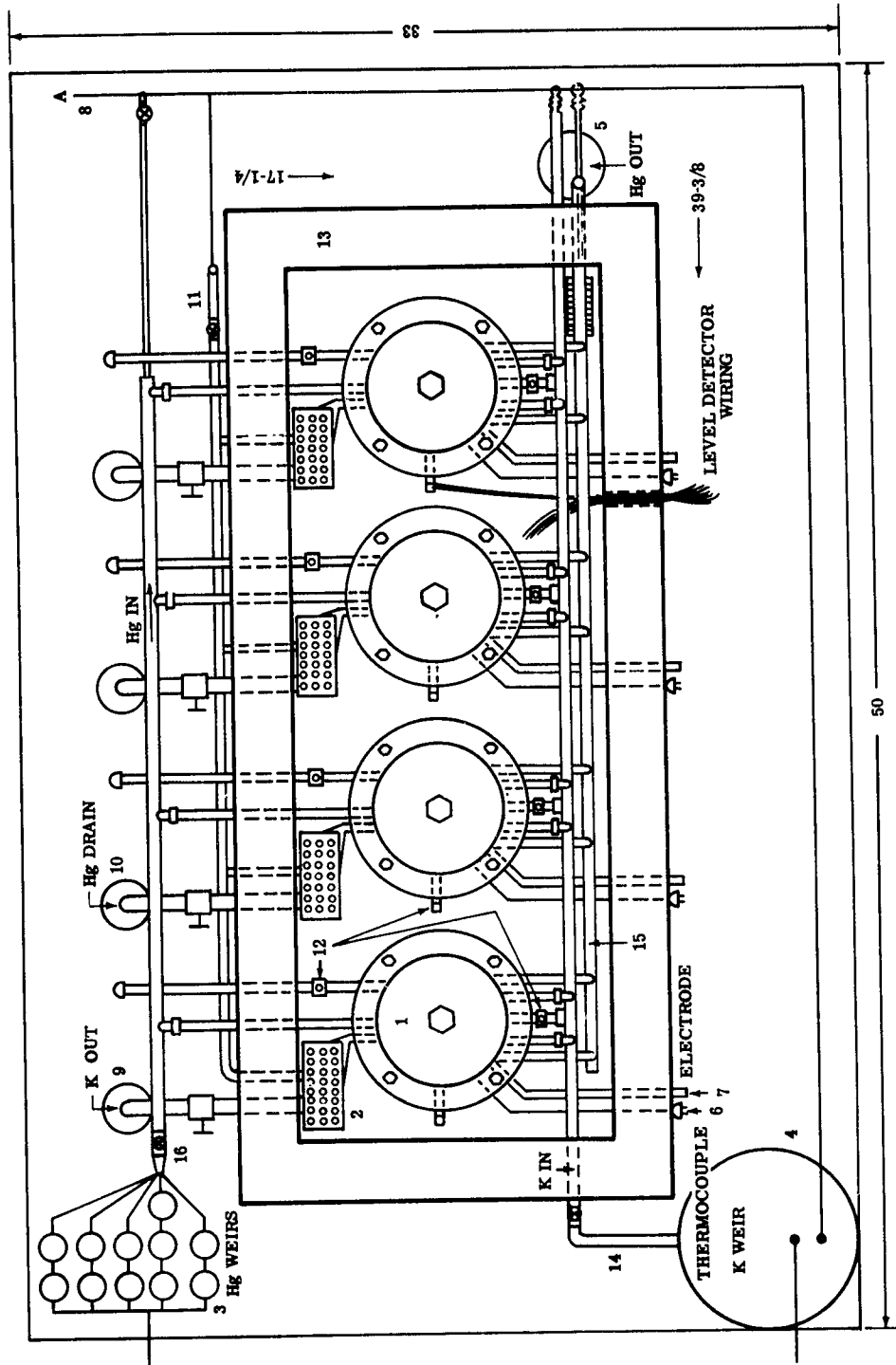


Figure 32. Top View of 310-Watt Stack of 3-in. Cells

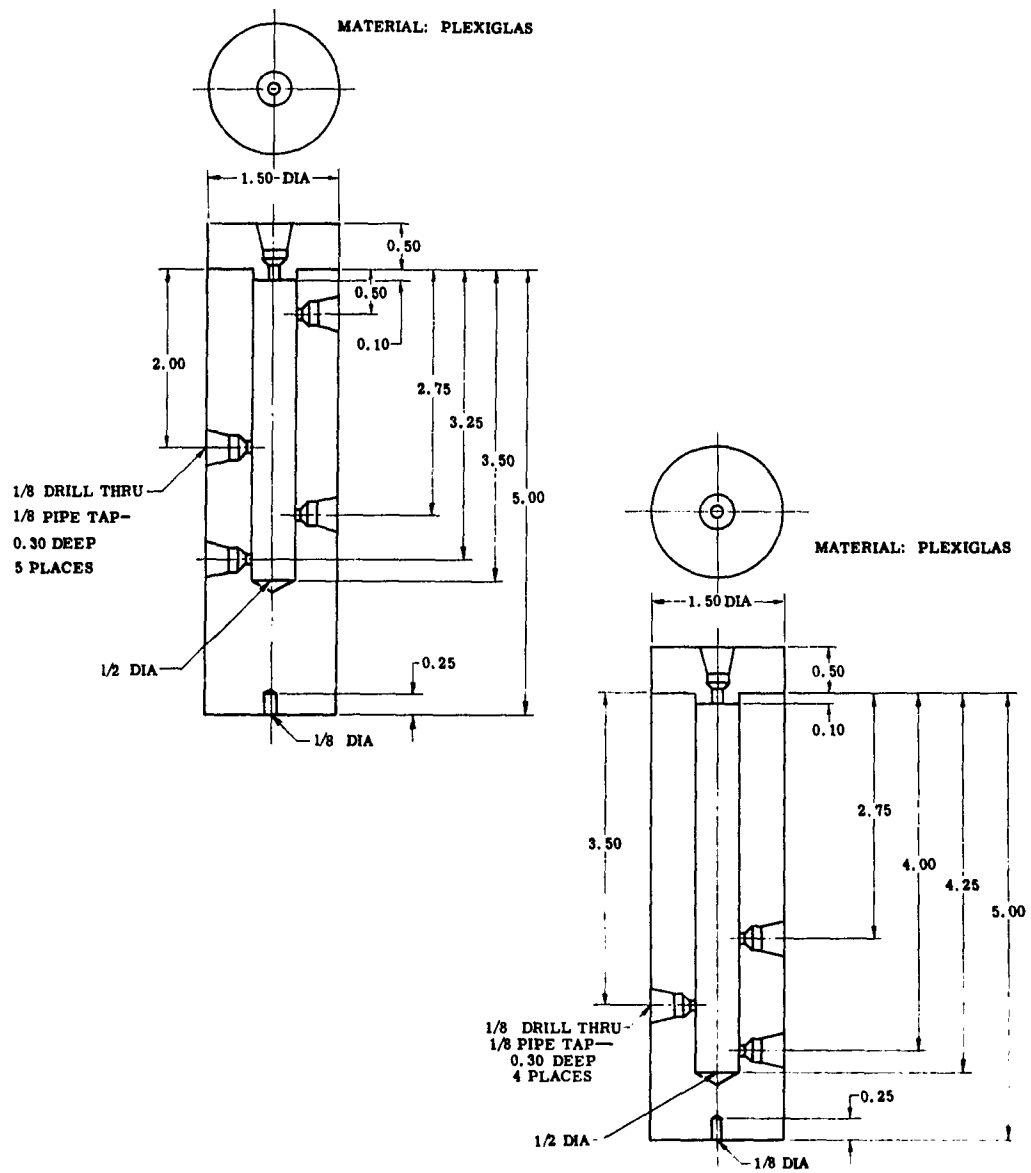


Figure 33. Detail of Mercury Weirs

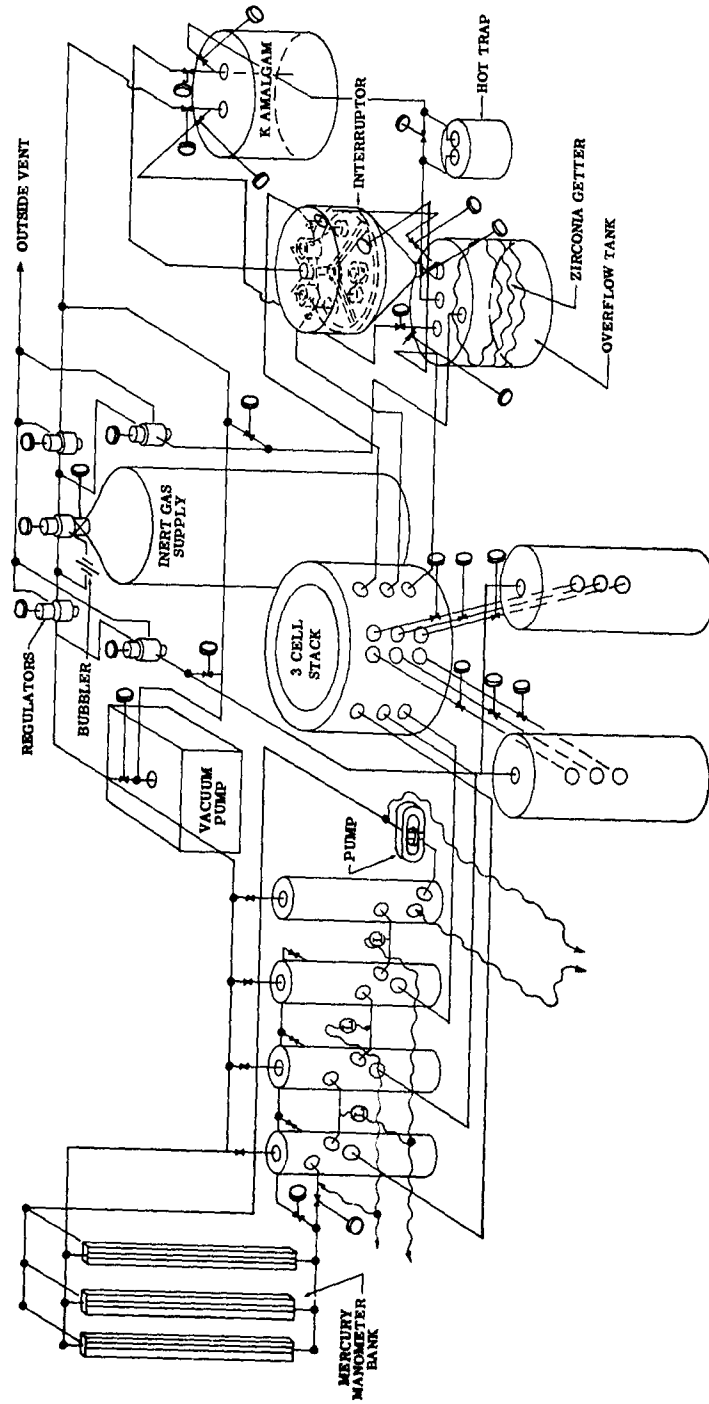


Figure 34. Schematic of Feed System for Liquid Metal Cell Stack

feed system for the full stack. The weirs are used for control of the hydrostatic heads of mercury going into any particular horizontal layer of cells, eliminating the possibility of flexural damage to the matrix and minimizing the possibility of hydrostatic pressure forcing electrolyte from the pores. Each weir will have an upper and lower section serving a different layer of cells. A pipe from a weir to a particular layer will feed through one of the mercury feed manifolds, No. 16.

- No. 4 is a totally enclosed and inerted potassium feed weir (Figure 35).
- No. 5 indicates the collection pot for the mercury-rich amalgam feeding out of the cells through the mercury effluent manifold and collection weir (just inside the furnace). The mercury effluent manifold is indicated by No. 15. All manifolds in this system will be hooked to the cells by easily disconnectable joints so that if during operation a cell short should occur, the offending cell can be quickly disconnected from electrical parallelism, which would confine the loss to 5 watts. Otherwise, shorting of any one cell would result in a power loss of 20 watts.
- No. 6 indicates thermocouple outlets on the outside of the oven. There will be four thermocouples in each column of 21 cells—one located near the top, one located near the bottom, and two located near the center.
- No. 7 indicates the electrode leads coming to the outside from each cell. The leads in any particular layer will be connected externally to a bus bar, as shown in the schematic of the electrical system (Figure 36).
- No. 8 indicates an argon manifold. This manifold is tied into all the feed and effluent manifolds in the system so that, if it is desired to disconnect a particular cell, the valve linking the feed weir to a particular manifold can be closed. To clear the manifold, the valve admitting argon to the manifold can be opened and the material within the manifold forced into the cells. While still under positive pressure, the



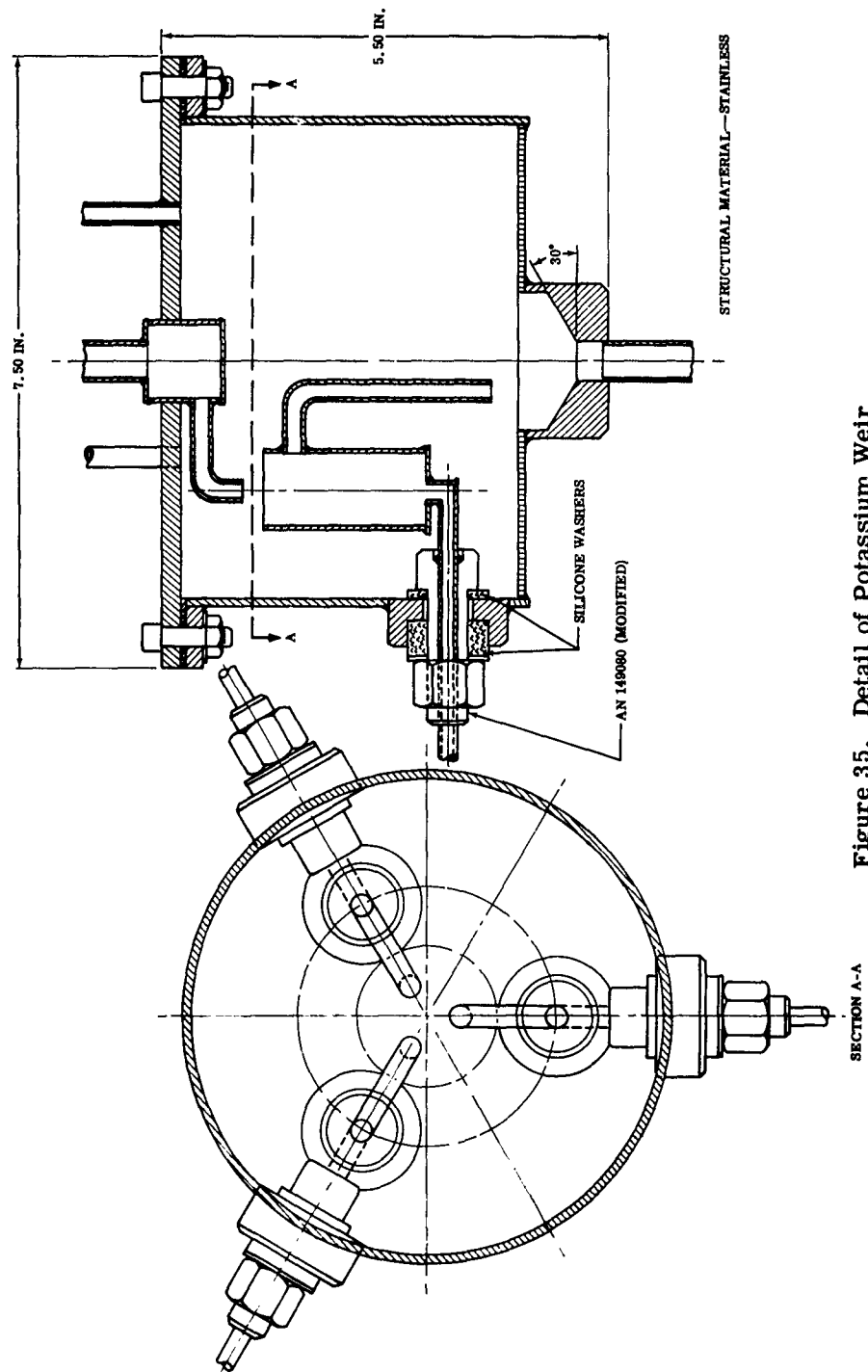


Figure 35. Detail of Potassium Weir

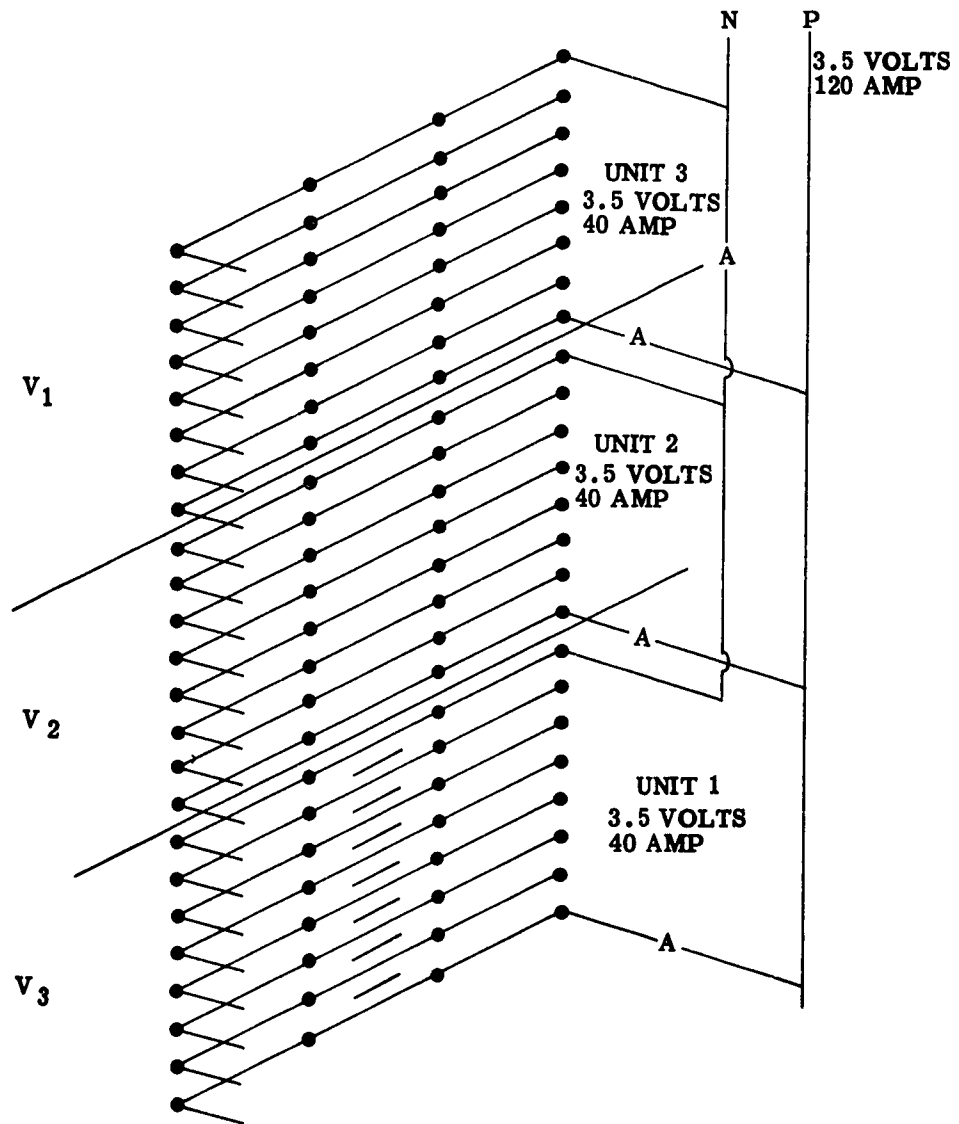


Figure 36. Schematic of Exterior Electrical Connections



disconnection would be made and the joints would be capped. At this point the argon pressure would be reduced and feed for the other three cells would be restarted from the feed weir. The argon line will also serve to sweep out the cell before loading so that the last traces of air can be removed before the mercury or amalgams are loaded.

- No. 9 is the single drain from each of the collector-interrupters for the amalgam.
- No. 10 indicates the drains from the mercury side of the cell.
- No. 11 is the argon manifold which inerts the collector-interrupters.
- No. 12 indicates the three electrical level gauges previously mentioned.
- No. 13 is the furnace wall.
- No. 14 is the potassium feed manifold.
- No. 15 is the mercury effluent manifold.
- No. 16 is the mercury feed manifold.

It should be mentioned that if a short occurs through a matrix, it would not be necessary to disconnect the cell from the manifolds. The short could be interrupted merely by opening the mercury drain for that particular cell and allowing the mercury going into the cell to drain out rather than establishing contact with the matrix.

The feed system schematic shown in Figure 34 shows the argon source to be used in the cell layers or manifolds to pressure feed each of the weirs. The potassium would go from the initial potassium melting pot into the potassium weir and would overflow into the collection pot which contains zirconium

metal, an oxygen getter. It is proposed that, before operation is begun, a full batch of potassium be purified by running it through the collection pot, pumping it back up to the feed tank and a hot trap, and then through the weirs into the cells. On the mercury side, prior to being fed into the weirs, the mercury can be vacuum degassed, removing any entrained air or moisture. It will then go from the feed tank into the weirs and then into the cells.

A detail drawing of the potassium weir is shown in Figure 35 (shown as No. 4 in Figure 32).

The schematic of the electrical system in Figure 36 shows the connections to the bus bars on the exterior of the furnace. The seven cells in Unit 1 would be in electrical series, as would the cells in Units 2 and 3. Each dot represents one of the four cells across the width of the furnace. The three units would be connected in parallel to produce 3.5 volts and 420 watts. One ammeter and a selector switch will be used to monitor the current output for the stack as a whole or the current output from each of the three units. One voltmeter will continuously monitor the stack voltage; a separate voltmeter will monitor the voltage within each unit, and, by means of a selector switch, voltages can be measured either across the whole unit or between any two cells in the unit.

Designs for the circular cell stack will be completed during the next report period and a design will be laid out for a larger cell, most likely of the rectangular type. The rectangular stack design would use the same feed system as proposed for the circular stack.

#### MULTICELL UNIT FABRICATION

To gain experience with the proposed stack and feed system, a three-cell unit and press is being fabricated. Initial work with this unit will consist of tabletop tests at room temperature utilizing mercury on the mercury side



and salt water on the amalgam side to simulate the potassium-mercury amalgam. Any needed changes or improvements will be indicated by these tests--- the three-cell unit will then be run in the furnace as a 1.5-volt cell. Upon successful completion of this test, a second test is proposed in which the press now available and the press under construction will be used with a single cell unit and an intermediate unit. In effect, two parallel one-volt units of two cells each will be tested so that manifold feeding and disconnecting can be evaluated. These two experiments should yield enough information to permit fabrication of the full stack.

## VI. TECHNICAL POSITION

The schedule for the liquid metal cell program is shown in Figure 37. Task IA is complete for both circular- and rectangular-type cells. Task IB is approximately ten days behind schedule to allow for improvement of the cell sealing technique.

Circular Cell---Work is approximately one week behind schedule to allow for improving the sealing technique. In the month available prior to adoption of final design (1 May 1962), operation of the single cell and a three-cell unit lends sufficient time to evaluate the LA-830 matrix and do the other experimentation necessary to increase the wattage to the desired five watts.

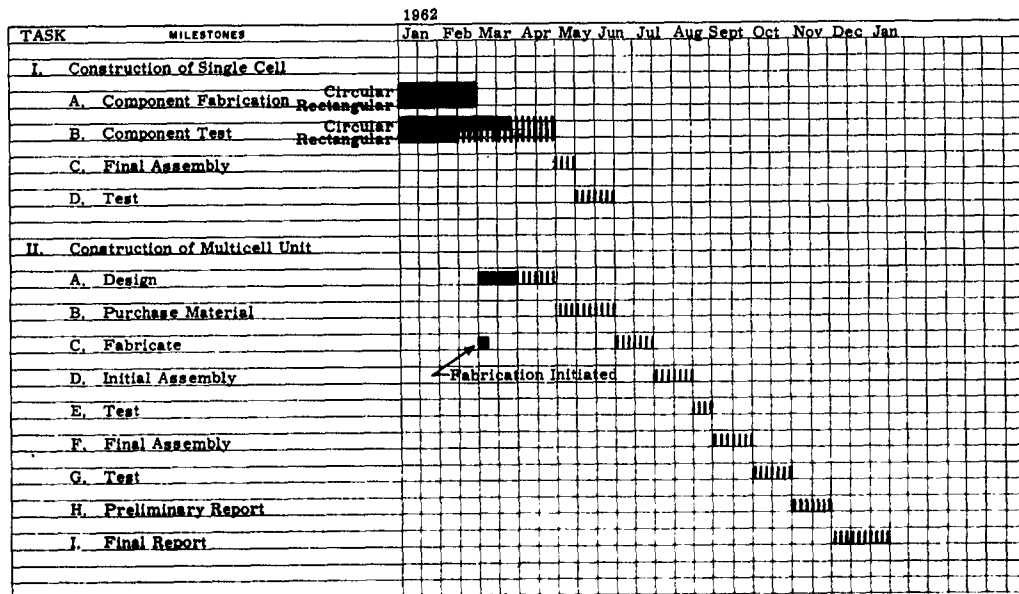


Figure 37. Program Schedule



**ALLISON**

---

Rectangular Cell—Component fabrication is completed. All test equipment is ready. Conversation with the manufacturer at the date of this writing indicated that the alumina frame has completed the first firing successfully (this is the firing in which most shrinkage takes place and there is the most danger of cracking) and is being machined prior to the high temperature firing. Delivery was indicated in one and one-half weeks. The rectangular matrix built at Allison is in the process of being sealed—delivery is expected within one week.

Multicell Design—This work is on schedule. It is expected that preliminary design of the circular stack will be completed within the first week of the next reporting period, and the preliminary feed systems will then be applied to the rectangular stack.

Multicell Fabrication—This work is well ahead of schedule for the circular cell. Two presses are in existence with three single cells and two intermediate cells. Experience gained in fabrication of these units should expedite production of additional units in the shop.

## VII. WORK PLAN FOR NEXT REPORT PERIOD

During the second quarter it is intended to complete single cell testing of the circular cells; to make whatever corrections are necessary in the handling technique or matrix design to eliminate the high resistances encountered to date; and to improve the power output to the desired five-watt level. Hot testing of the three-cell stack and the two two-cell units will be completed and the necessary evaluations made for the design of the complete stack. Additionally, it is intended to run a single cell with an 81-cm<sup>2</sup> matrix, the successful operation of which would enable the cell stack and the preliminary design to be cut in half. This stack would consist of only two columns of 21 cells each. Upon delivery of the finished picture frame matrices, the rectangular cell will be evaluated. If this evaluation can be completed in time for the building of a stack around this concept, work on the circular cell will be dropped and the alternate path with larger cells will be followed.

Preliminary designs will be completed and a final design and drawings will be worked out. Emphasis during the second quarter will be to reduce the weight and volume of the stack as much as possible without departing from known designs that have been evaluated. Arrangements have been made as of this date for the expeditious purchase of needed materials and no problem is seen in the on-time fabrication of the cell stack.

It is expected that by the end of the second quarter, the stack will be ready for initial assembly, Task IID.



# I

---

## VIII. REFERENCES

1. Weaver, R. D. and Shriver, E. L. The Fuel Cell Literature. Allison Division, General Motors Corporation. APS 10 (1959).
2. Yeager, E. in Proceedings of the 12th Annual Battery Research and Development Conference. Asbury Park, New Jersey (1958) pp 2-4.
3. Caple, W. G. and Shriver, E. L. Thermally Decomposable Inorganic Compounds. Allison Division, General Motors Corporation. ACS 1 (1960).
4. King, J. Jr. and others, in Energy Conversion for Space Power. New York, Academic Press, 1961, pp 387-410.
5. Henderson, R. E., Agruss, B., and Caple, W. G. ibid. pp 411-423.
6. Laitinen, H. P. A. and others, in Journal of the Electrochemical Society. Vol. 107 (1960) pp 546-555.
7. Kubaschewski, O. and Evans, E. L. Metallurgical Thermochemistry. New York, Pergaman Press, 1958, pp 6-72.
8. Selected Values for the Thermodynamic Properties of Metals and Alloys. Research Laboratory, Institute of Engineering Research, University of California, Berkeley, California (1959).
9. Liquid Metals Handbook. Atomic Energy Commission, Department of the Navy, Washington, D.C. (June 1950).
10. Handbook of Chemistry and Physics. 30th Edition. Cleveland, Ohio, Chemical Rubber Publishing Co., 1948.



11. Metals Handbook. American Society for Metals (1948).
12. Oxide Ceramics. New York, Academic Press, 1960.
13. Smith, T. P. Corrosion of Materials in Fused Hydroxides. Oak Ridge National Laboratories, Oak Ridge, Tennessee.
14. The Norton Company, Worcester, Massachusetts.
15. Whittemore, O. J. and Ault, N. N. in Journal of American Ceramics Society. Vol. 39 (1956) p 443.
16. Benesi, H. A. and others. "Pore Volume of Solid Catalysts by Carbon Tetrachloride Absorption." Analytical Chemistry. Vol. 27 (1955) p 1963.
17. Mantell, C. L. Engineering Materials Handbook. New York, McGraw-Hill Book Co., Inc., 1958.
18. NASA-AEC Liquid Metals Corrosion Meeting. NASA-TDN 769. Washington, D.C. 1961.
19. Mellor, T. A Comprehensive Treatise on Inorganic and Theoretical Chemistry. New York, Longmans-Green, 1956.
20. International Critical Tables. Washburn, ed. Vol. 4, 1920.

<p>Allison Division, General Motors Corporation FIRST QUARTERLY TECHNICAL PROGRESS REPORT ON DESIGN AND DEVELOPMENT OF A LIQUID METAL CELL FOR THE PERIOD 1 JANUARY 1942-31 MARCH 1942. 15 April 1942. 68 p. incl. illus. (Project No. 3145, Task No. 60813) (Allison EDR 2878) (Contract AF33(657)-7847)</p> <p>Electrochemical, physical, and chemical characteristics of potassium, mercury, and potassium-mercury amalgams lend themselves to the successful operation of a liquid metal cell for space power. Construction of single liquid metal cells and a three-cell unit are complete and testing is in progress. Preliminary design work to show that the cells can be combined into a system which will function as a battery are nearly complete. Photographs and detailed drawings of the units used for the cell, instrumentation, feed system, etc. are shown.</p>	<ol style="list-style-type: none"> <li>1. Liquid Metals</li> <li>2. Thermal Regeneration</li> <li>3. Energy Conversion</li> <li>1. Dr. B. Agras</li> <li>II. H. R. Karas</li> <li>III. Flight Accessories</li> <li>IV. Laboratory, ASD</li> </ol> <p>Contract AF33(657)-7847</p>
--	--

<p>Allison Division, General Motors Corporation FIRST QUARTERLY TECHNICAL PROGRESS REPORT ON DESIGN AND DEVELOPMENT OF A LIQUID METAL CELL FOR THE PERIOD 1 JANUARY 1942-31 MARCH 1942. 15 April 1942. 68 p. incl. illus. (Project No. 3145, Task No. 60813) (Allison EDR 2878) (Contract AF33(657)-7847)</p> <p>Electrochemical, physical, and chemical characteristics of potassium, mercury, and potassium-mercury amalgams lend themselves to the successful operation of a liquid metal cell for space power. Construction of single liquid metal cells and a three-cell unit are complete and testing is in progress. Preliminary design work to show that the cells can be combined into a system which will function as a battery are nearly complete. Photographs and detailed drawings of the units used for the cell, instrumentation, feed system, etc. are shown.</p>	<ol style="list-style-type: none"> <li>1. Liquid Metals</li> <li>2. Thermal Regeneration</li> <li>3. Energy Conversion</li> <li>1. Dr. B. Agras</li> <li>II. H. R. Karas</li> <li>III. Flight Accessories</li> <li>IV. Laboratory, ASD</li> </ol> <p>Contract AF33(657)-7847</p>
--	--

<p>Allison Division, General Motors Corporation FIRST QUARTERLY TECHNICAL PROGRESS REPORT ON DESIGN AND DEVELOPMENT OF A LIQUID METAL CELL FOR THE PERIOD 1 JANUARY 1942-31 MARCH 1942. 15 April 1942. 68 p. incl. illus. (Project No. 3145, Task No. 60813) (Allison EDR 2878) (Contract AF33(657)-7847)</p> <p>Electrochemical, physical, and chemical characteristics of potassium, mercury, and potassium-mercury amalgams lend themselves to the successful operation of a liquid metal cell for space power. Construction of single liquid metal cells and a three-cell unit are complete and testing is in progress. Preliminary design work to show that the cells can be combined into a system which will function as a battery are nearly complete. Photographs and detailed drawings of the units used for the cell, instrumentation, feed system, etc. are shown.</p>	<ol style="list-style-type: none"> <li>1. Liquid Metals</li> <li>2. Thermal Regeneration</li> <li>3. Energy Conversion</li> <li>1. Dr. B. Agras</li> <li>II. H. R. Karas</li> <li>III. Flight Accessories</li> <li>IV. Laboratory, ASD</li> </ol> <p>Contract AF33(657)-7847</p>
--	--

<p>Allison Division, General Motors Corporation FIRST QUARTERLY TECHNICAL PROGRESS REPORT ON DESIGN AND DEVELOPMENT OF A LIQUID METAL CELL FOR THE PERIOD 1 JANUARY 1942-31 MARCH 1942. 15 April 1942. 68 p. incl. illus. (Project No. 3145, Task No. 60813) (Allison EDR 2878) (Contract AF33(657)-7847)</p> <p>Electrochemical, physical, and chemical characteristics of potassium, mercury, and potassium-mercury amalgams lend themselves to the successful operation of a liquid metal cell for space power. Construction of single liquid metal cells and a three-cell unit are complete and testing is in progress. Preliminary design work to show that the cells can be combined into a system which will function as a battery are nearly complete. Photographs and detailed drawings of the units used for the cell, instrumentation, feed system, etc. are shown.</p>	<ol style="list-style-type: none"> <li>1. Liquid Metals</li> <li>2. Thermal Regeneration</li> <li>3. Energy Conversion</li> <li>1. Dr. B. Agras</li> <li>II. H. R. Karas</li> <li>III. Flight Accessories</li> <li>IV. Laboratory, ASD</li> </ol> <p>Contract AF33(657)-7847</p>
--	--